Immobilized Enzymes: Activity, Orientation, and Stability

By

McKenna M. Schroeder

A dissertation submitted in partial fulfillment
of the requirements for the degree of
Doctor of Philosophy
(Chemical Biology)
in the University of Michigan
2017

Doctoral Committee:

Professor E. Neil G. Marsh, Chair
Assistant Professor Julie S. Biteen
Professor Zhan Chen
Associate Professor Bruce A. Palfey

Table of Contents

List of Figures

List of Tables

Abstract

Enzyme immobilization is an important tool for many industrial and medical fields applications as well as biosensors. Much work has been done developing types of immobilization, yet the field lacks a comprehensive understanding of the relationship between immobilized enzyme orientation and activity/stability. This work was done to build a more complete picture of the interplay between activity, stability, orientation, and surface characteristics for immobilized enzymes.

In Chapter 2, we started by making uniform, chemically defined self-assembling monolayer (SAM) surfaces functionalized with maleimide to bind NfsB through single cysteine residues. Two orientation NfsB constructs were used in these experiments, H360C and V424C. Orientation was not found to change the specific activity.

In Chapter 3, SAM surfaces functionalized with EG_3-MAL, EG_3-OH and EG_3-ME terminated linkers were made to explore the effects of surface characteristics on immobilized NfsB. We found that for mixed surfaces a mole ratio of 1:10 EG_3-MAL:EG_3-OH and EG_3-MAL:EG_3-ME resulted in a significantly higher specific activity compared to a 1:1 or 1:20 mole ratio. In these experiments, T ½ was used as a measure of thermal stability. T ½ was increase , but was unaffected by orientation. Mixed surfaces with both EG_3-ME and EG_3-OH with EG_3-MAL held at a constant concentration were created. These mixed surfaces were used to explore the relationship between surface hydrophobicity and the activity/stability of the

immobilized enzyme. T ½ was unaffected by surface hydrophobicity while specific activity nearly doubled from 100% EG_3-ME surface to 100% EG_3-OH surface. A variant of NfsB was created placing the cysteine on an α-helix. The α-helix anchor site didn't change the specific activity or T ½ of immobilized NfsB.

The experiments described in Chapter 4 were performed to investigate the effect of surface crowding on specific activity and stability of immobilized NfsB. Multiple surface coverage conditions from a sparse monolayer to a densely packed monolayer were used for activity and T ½ measurements. Two NfsB variants V424C and S63C showed no change in specific activity or T ½ arising from changes in surface density. NfsB-H360C showed a decrease in specific activity and T ½ at lower surface density.

Chapter 1

Introduction

1.1 Introduction

Enzymes are unmatched in their ability to catalyze reactions and achieve remarkable rate acceleration and specificity. Life would not be possible without enzymes. Enzymes take reactions that would otherwise proceed extremely slowly or not at all, proceed at rates that are relevant on a biological timescale. As an extreme example, the decarboxylation of orotic acid[1] has a half-time of 78 million years but orotidine 5'-phosphate decarboxylase increases the rate by a factor of 10^{17}. A more typical example is the deamination of adenosine which is critical for the turnover of nucleic acids. Without catalysis the reaction would proceed with a half-time of 120 years[1]. Adenosine deaminase enhances the rate of reaction by a factor of 10^{12}. Beyond the remarkable rate enhancements, enzymes typically catalyze reactions with stereospecificity that would in most cases be difficult to achieve using conventional synthesis techniques. Additionally enzymes

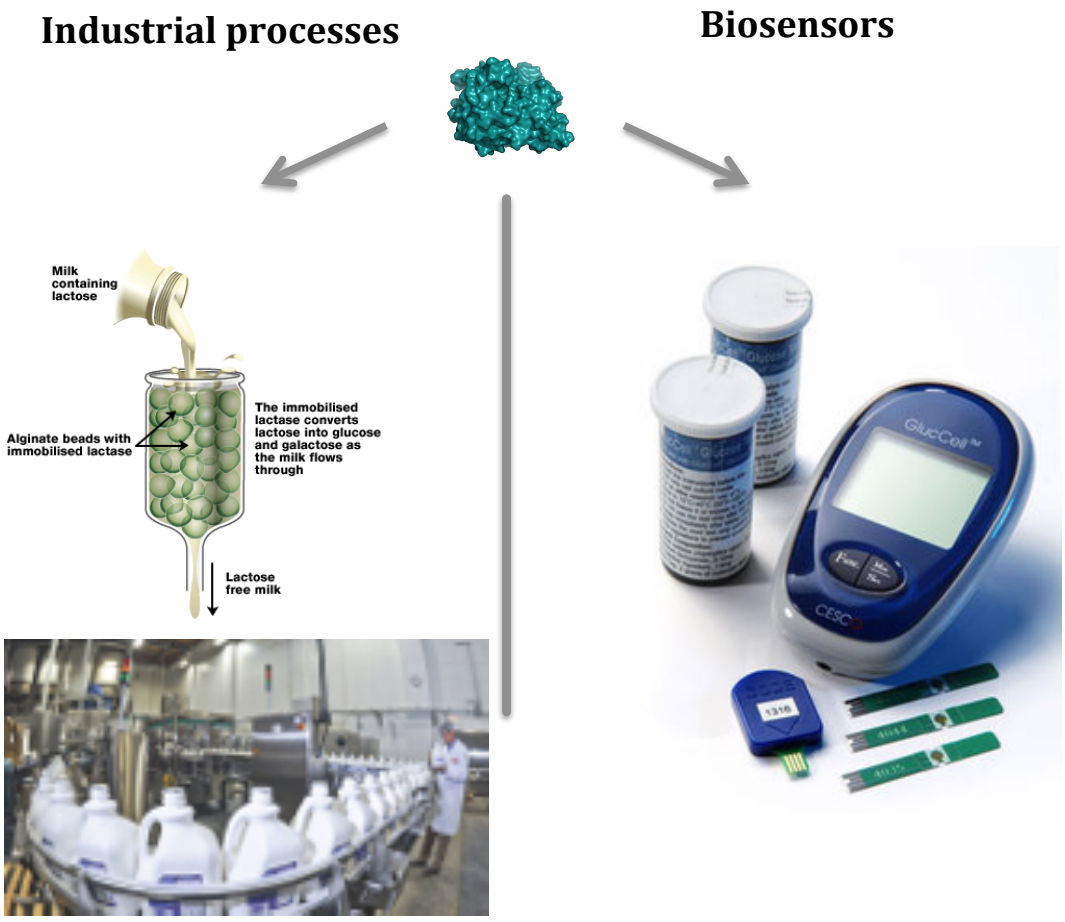

Figure 1.1 Examples of Immobilized Enzyme Applications
Lactose being removed from milk using lactase (left) and blood glucose meter (right).

are highly substrate-specific and operate under mild conditions of temperature, pressure and pH which are desirable for large-scale production. Taking all these qualities into consideration, enzymes are potentially extremely powerful tools for industrial chemical transformations or applications as biosensors (Figure 1.1).

Despite their catalytic power, there are important limitations to using enzymes in industrial or medical settings. As catalysts, enzymes are inherently reusable; however, using enzymes in aqueous solution as homogenous catalysts means that reuse is not always feasible or economical because of the difficulty of re-purification steps. Product or substrate inhibition can also limit the ability of an enzyme to catalyze reactions to completion in a conventional batch reaction. Another drawback is that some enzymes can be quite expensive to express and purify, so facilitating easier re-use presents an economic advantage. Enzyme immobilization on a solid support is one method for overcoming these limitations.

1.2 Immobilized Enzyme Applications

Immobilizing an enzyme on a solid support has a number of advantages in a commercial, medical, or industrial setting. Immobilization facilitates the removal of enzyme from a reaction and simplifies re-purification procedures. This fundamentally simplifies the reuse of enzymes, thereby increasing the efficiency and reducing the cost. Immobilized enzymes can be used in flow reactors to allow

continuous operation and reduce product inhibition effects[2]. Immobilized enzymes also make highly selective biosensors[3]. Clearly the power of immobilized enzymes can be applied in many settings.

Immobilized enzymes are important in a number of commercial food processing applications where their lack of toxicity is important. For example, pectin is an undesirable component in the production of fruit juices. The mixture of polysaccharides that makes up a major part of plant cell walls also causes juice to be turbid and contain solid suspensions. The removal of these undesirable components is necessary in the processing of fruit juices. Pectin lyase, an enzyme that degrades pectin, is used in this process. Pectin lyase has been immobilized to a variety of solid supports, including alginate gel[4], nylon[5,6], porous glass[7] and DEAE cellulose[7], to be used commercially in this process.

High fructose corn syrup (HFCS) is produced in massive quantities by the food industry as this ingredient is used increasingly in foods and beverages as an inexpensive sweetener. $1x10^7$ tons of HFCS are produced per year[8]. The production of HFCS is one of the most important uses of immobilized enzyme in the food industry. The process uses immobilized glucose isomerase in a final step to convert glucose to fructose[9]. This reaction scheme is shown in Figure 1.2. There are four main types of immobilized glucose isomerase used commercially, adsorbed on anion-exchange resin, adsorbed on SiO_2, or polyethyleneimine-treated alumina[9]. Immobilization on DEAE-cellulose results in a system with

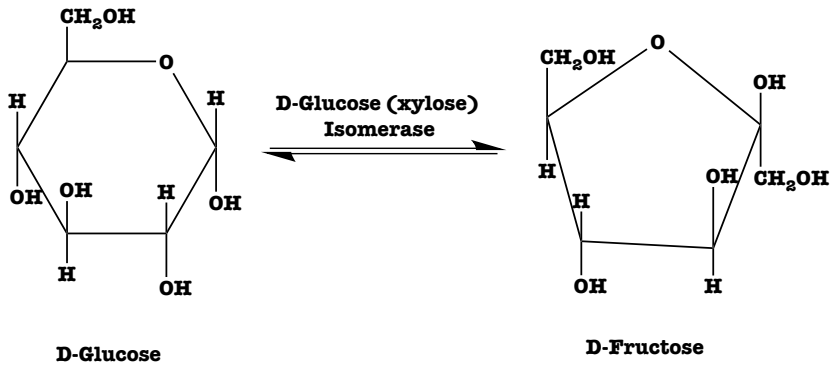

Figure 1.2 Glucose Isomerase
Scheme for reaction catalyzed invitro by glucose isomerase. Adapted from *Microbiol. Rev.* **60,** 280–300 (1996)

exceptional flow characteristics that support continuous operation of the reactors. When immobilized on alumina, the enzyme's cofactor, Co^{2+}, can be co-immobilized with the enzyme. This is advantageous because it eliminates the need to add Co^{2+} to the reaction mixture.

Immobilized enzymes also play an important role in the field of biosensors, which exploits their high substrate specificities to create highly selective biosensors. There are many examples of biosensors that utilize immobilized enzymes[3,10–12]. Carnitine is a substance that is involved in fat metabolism that is made in the liver and kidneys. The measurement of serum levels of carnitine is used to diagnose deficiencies. In a coupled system, serum carnitine can be detected spectroscopically using immobilized carnitine dehydrogenase and diaphorase[13]. The reaction is

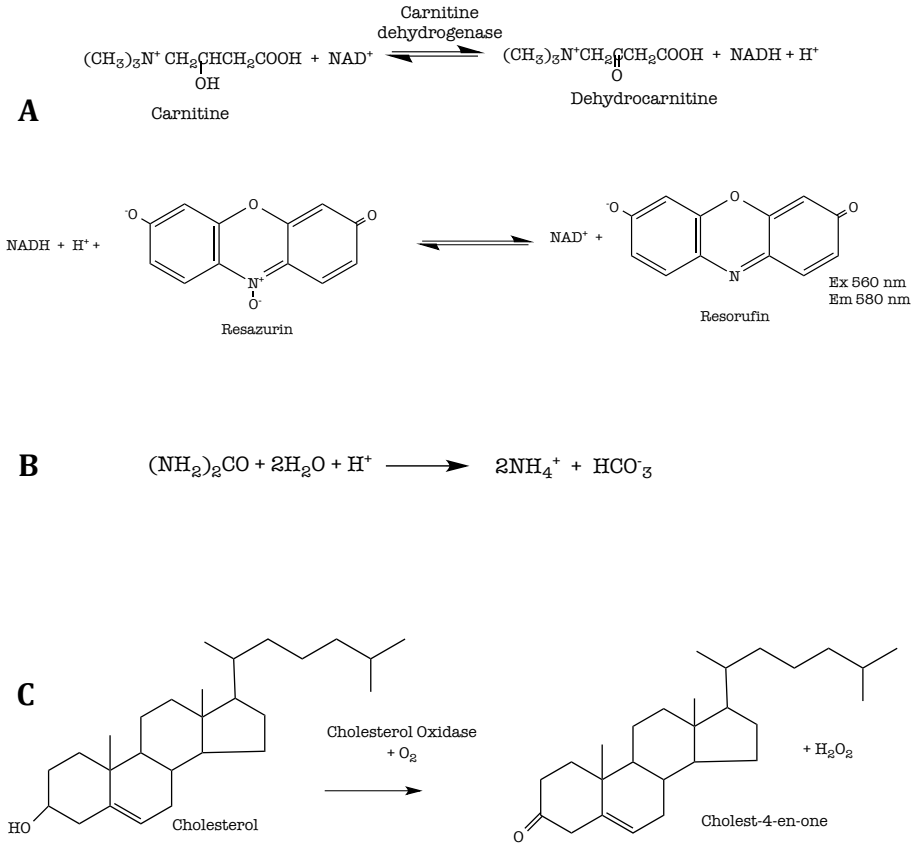

Figure 1.3 Reaction Schemes for Various Biosensors

A) Reaction scheme for determination of carnitine using carnitine dehydrogenase and diaphorase adapted from *Clin. Chem.* **36,** 2072–2076 (1990) . B) Reaction Scheme for detection of urea by urease. C) Scheme for enzymatic oxidation by cholesterol oxidase, adapted from *Analyst* **119,** 2331–2336 (1994)

shown in Figure 1.3 A. An important test for kidney function is performed by measuring the urea concentration present in blood samples. A disposable biosensor for urea using immobilized urease was developed by Eggenstein and co-workers[14]. Their biosensor uses an electrode coated in immobilized urease. As urea is hydrolyzed by the immobilized enzyme NH_4^+ is created (Figure 1.3 B) and detected by the electrode. Immobilized cholesterol oxidase is used as a biosensor for cholesterol by immobilizing the enzyme in a cellulose acetate membrane[15]. The reaction is shown in Figure 1.3 C. H_2O_2 is measured amperometrically and correlated to cholesterol concentration. This enzyme-based cholesterol biosensor is fabricated reliably and inexpensively resulting in a sensor with high sensitivity.

Perhaps the most important example of an immobilized enzyme biosensor is the blood glucose meter. At least 21 million people in the United States currently have diabetes according to the Centers for Disease Control and Prevention, although the real number is likely higher as many people go undiagnosed. A critical piece of equipment necessary to manage this disease is the blood glucose meter used to monitor blood sugar levels. There are four types of glucose biosensors, the most common based on glucose oxidase. The glucose oxidase is immobilized in a polymer layer in the test strip and coupled with a platinum electrode. When the blood sample is added the glucose oxidase catalyzes the oxidation of glucose by oxygen. The reaction scheme is shown in Figure 1.4. The resulting flow of electrons is proportional to the amount of glucose present in the blood sample[16]. This signal is

A $\text{Glucose} + \text{GOx} - \text{FAD}^+ \rightarrow \text{Glucolactone} + \text{GOx} - \text{FADH}_2$

B $\mathbf{GOx - FADH_2 + O_2 \rightarrow GOx - FAD + H_2O_2}$

C $H_2O_2 \rightarrow 2H^+ + O_2 + 2e$

Figure 1.4 Reaction Schemes for Blood Glucose Detection
A) Reaction scheme for the oxidation of glucose by glucose oxidase. B) Cofactor regeneration by reaction with oxygen forming hydrogen peroxide. C) Hydrogen peroxide is oxidized catalytically at anode, electron flow proportional to glucose. Adapted from *Sensors* **10,** 4558–4576 (2010).

then transduced into a read-out on the glucose meter. This is an outstanding example of the power of immobilized enzymes being used in a biosensor. The immobilized enzyme-based glucose test was a major advancement on its predecessor, which was a dye-based assay with significantly less sensitivity and accuracy than the enzyme-based test. This example captures the advantages of enzyme immobilization. Immobilization allows the assay to be embedded in the test strip and for the immobilized enzyme in the test strip to remain stable for a long time under varying conditions.

1.3 Types of Enzyme Immobilization

1.3.1 Physical Adsorption

There are various methods for immobilizing enzymes. Enzymes can be

trapped in a porous support, physically adsorbed or covalently bound[17]. Physical adsorption is perhaps the simplest form of immobilization, as it does not require any prior modifications to the enzyme. A diagram of physical adsorption of enzymes is shown in Figure 1.5. The binding process is also simple; it typically consists of an incubation period with the enzyme and solid support in buffer. Excess un-adsorbed enzyme is removed by washing the support with buffer.

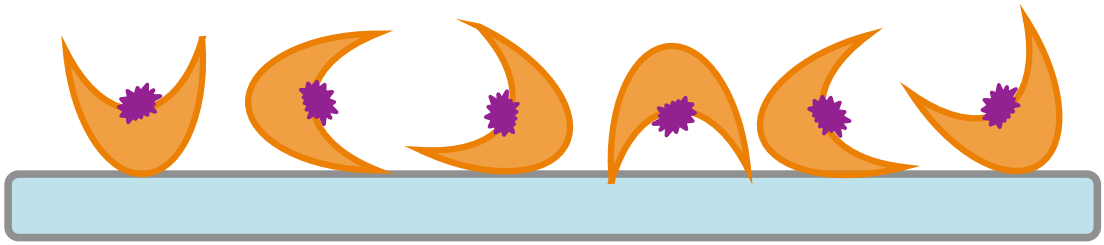

Figure 1.5 Diagram of Physical Adsorption
Diagram of enzyme physically adsorbed to solid support. Support represented in blue, enzyme represented in orange, active site represented in purple.

In physical adsorption the enzyme is bound to the support through weak interactions including Van der Waal's forces, hydrophobic and electrostatic interactions. These weak binding interactions are desirable because interactions that are too strong can distort the enzyme structure and reduce activity significantly[18-19]. On the other hand, the nature of these weak interactions makes enzymes immobilized by adsorption susceptible to desorption or leaching of the enzyme from the support. This method is particularly unsuitable for certain applications that would expose the adsorbed enzyme to large changes in temperature, pH, or ionic strength. Immobilization by adsorption is not always

suitable for more harsh industrial applications because of leaching, however, adsorption is often used for biosensors.

One important aspect of enzyme adsorption is the choice of support. There are many types of supports that can be successfully used for enzyme adsorption that include organic, inorganic, and insoluble materials[20,19]. Inorganic supports include silica, metal oxides, hydroxyapatite and porous glass. Some organic supports include polyacrylamide, polypropylene, chitin and cellulose. An advantage to using organic supports is that they are easily chemically modified. It is important to note that not all enzymes will work with every support. A particularly exciting and recent advance in adsorption supports is the use of nanoparticles and nanotubes.

An example of an organic nanotoube support is polypyrrole (PPy). PPy is of notable interest for biosensor applications because it is a conducting polymer that can be used as an immobilizing matrix. PPy is easy to prepare and also has good stability and conductivity[20]. Ekanaykae and co-workers[21] used a novel means of fabricating a nanotube array of PPy to create an amperometric glucose biosensor with adsorbed glucose oxidase. A film of PPy nanotubes was fabricated on an electrode by electropolymerization. Glucose oxidase was then physically adsorbed to the prepared PPy coated electrode. The PPy nanotubes provided a higher surface area for the enzyme to adsorb and an increased binding affinity such that the researchers were able to use less enzyme in the fabrication process. The resulting biosensor was highly sensitive to glucose and had a linear range between 0.5 mM and 10 mM. The use of nanotubes in this case increased the enzyme adsorption

efficiency, thereby potentially reducing production costs. Furthermore, this nanotube design created the highest sensitivity of any glucose biosensor adsorbed to PPy[21].

An excellent example of nanoparticles being used as a support for immobilized enzymes is the use of zirconia nanopartices by Chen and coworkers[22]. In their studies, Tween 85 and erucic acid were used to modify the surface of the zirconia nanoparticles from hydrophilic to hydrophobic. A lipase was physically adsorbed onto the surface of the modified zirconia nanoparticles and used to resolve (R,S)-Ibuprofen. The activity of the immobilized lipase was compared to the activity of crude lipase powders. The immobilized lipase on erucic acid modified zirconia nanoparticles had over twice the specific activity of the crude powder. Furthermore, the erucic acid-modified nanoparticles had three times the activity of the Tween-modified nanoparticles. This study demonstrates how critical surface modification can be to the activity of immobilized enzyme.

1.3.2 Entrapment

Enzymes can be immobilized by being entrapped or encapsulated in a porous matrix. A diagram of immobilization by entrapment is shown in Figure 1.6. Entrapment is subject to very different set of limitations than the other types of

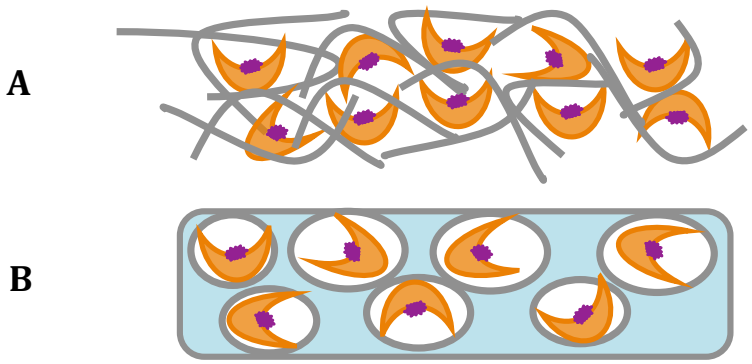

Figure 1.6 Diagram of Entrapment
Diagram of enzyme physically entrapped by a material such as polymer represented in grey (A) or entrapped in a porous material (B). Enzyme represented in orange, active site represented in purple.

immobilization, so it will only be discussed briefly. Similar to physical adsorption, entrapment is a relatively simple immobilization technique because it does not require modifications to be made to the enzyme itself. Enzyme entrapment is often associated with an increase in stability[23]. However, a major drawback of immobilization by entrapment is that it is frequently accompanied by a decrease in catalytic activity due to rate-limiting diffusion of substrate and products in and out of the encapsulating porous material.

Regardless of the drawbacks of entrapment, Sohail and Adeloju[24] successfully created a nitrate biosensor using nitrate reductase entrapped in PPy. Nitrate reductase was immobilized into PPy conducting films with β-NADH as the co-substrate. The co-encapsulation of the co-substrate with the enzyme significantly increased the sensitivity of the biosensor. Additionally, the use of the biosensor was made more efficient as only 0.3 mM NADH was necessary when co-encapsulated as

compared to 4 mM when NADH was added to the reaction solution. The biggest disadvantage for this electrode was the lack of reproducibility upon re-use. The authors proposed that this could be attributed to leaching of the enzyme or NADH from the PPy film during storage.

1.3.4 Covalent Immobilization

There are a variety of methods to covalently immobilize enzymes on solid supports. Typically, covalent methods take advantage of the reactivity of native functional groups on the enzyme's surface. A diagram of non-specific covalent immobilization by crosslinking is shown in Figure 1.7. These existing functional

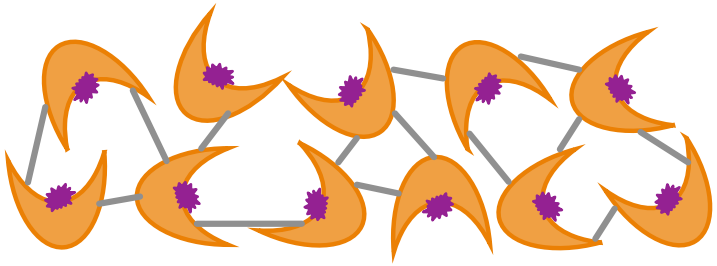

Figure 1.7 Diagram of Covalent Enzyme Immobilization
Diagram of non-specific enzyme immobilization by crosslinking. Bonds made by crosslinking reagents represented in grey. Enzyme represented in orange, active site represented in purple.

groups must not be important for activity of the enzyme otherwise the enzyme will be inactive once bound. Carboxyl groups on a support material can be bound to the amino groups on an enzyme using carbodiimides[23]. Epoxides can react with hydroxyl groups through a ring-opening reaction (Figure 1.8). N-hydroxy-succinimide can react with amine groups[25] (Figure 1.8). Glutaraldehyde is a

commonly used crosslinking reagent and can be used to crosslink reactive amine groups on an enzyme with each other or with inert proteins like bovine serum albumin. A reaction scheme of enzyme immobilization, on an aminated surface with carbodiimide or glutaraldehyde, is shown in Figure 1.9. These types of covalent enzyme attachments are simple to perform, proceed by efficient reactions, and reduce potential leaching of the immobilized enzyme from the solid supports. The main drawback of this type of immobilization is loss of enzyme activity[25]. The loss of catalytic activity is likely caused by distortion of the enzyme structure that impedes the function of the active site. Another cause of activity-loss might be attributed to an enzyme orientation resulting in complete blocking of the active site, denying entrance of substrate or exit of product.

A very interesting and successful example of the use of glutaraldehyde crosslinking was reported by Zhai and co-workers[26]. Their group fabricated a platinum nanoparticle polyaniline hydrogel heterostructure. Polyaniline is a conducting polymer similar to PPy discussed previously. Glucose oxidase was immobilized in the hydrogel structure electrode by glutaraldehyde crosslinking. The electrode was then used to measure glucose concentrations in PBS. They report their glucose sensor to have a sensitivity of 96.1 $\mu A\ mM^{-1}cm^{-2}$, which is 13 times higher sensitivity than the PPy nanotube based glucose sensor discussed previously. The authors propose that this increase in sensitivity is due to reduced diffusion length and improved charge transfer of this glucose sensor.

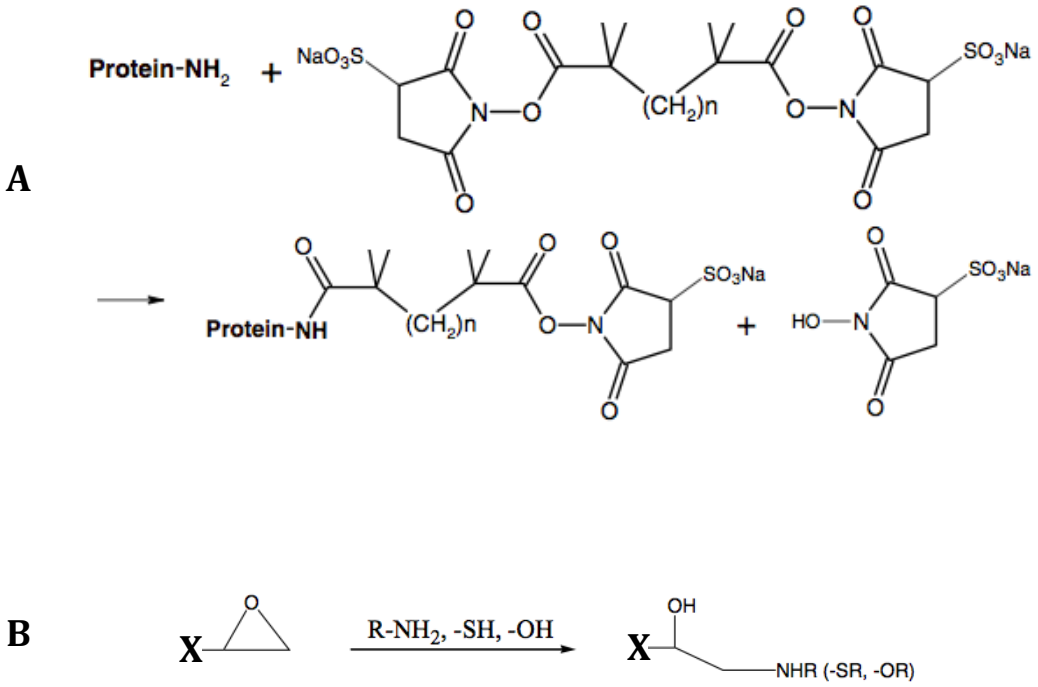

Figure 1.8 Reaction Scheme for N-hydroxy-succinimide and Epoxides
Immobilization reaction scheme with A) N-hydroxysuccinimide and a protein or B) epoxide, where x is the surface (adapted from *3 Biotech* 1–9 (2012))

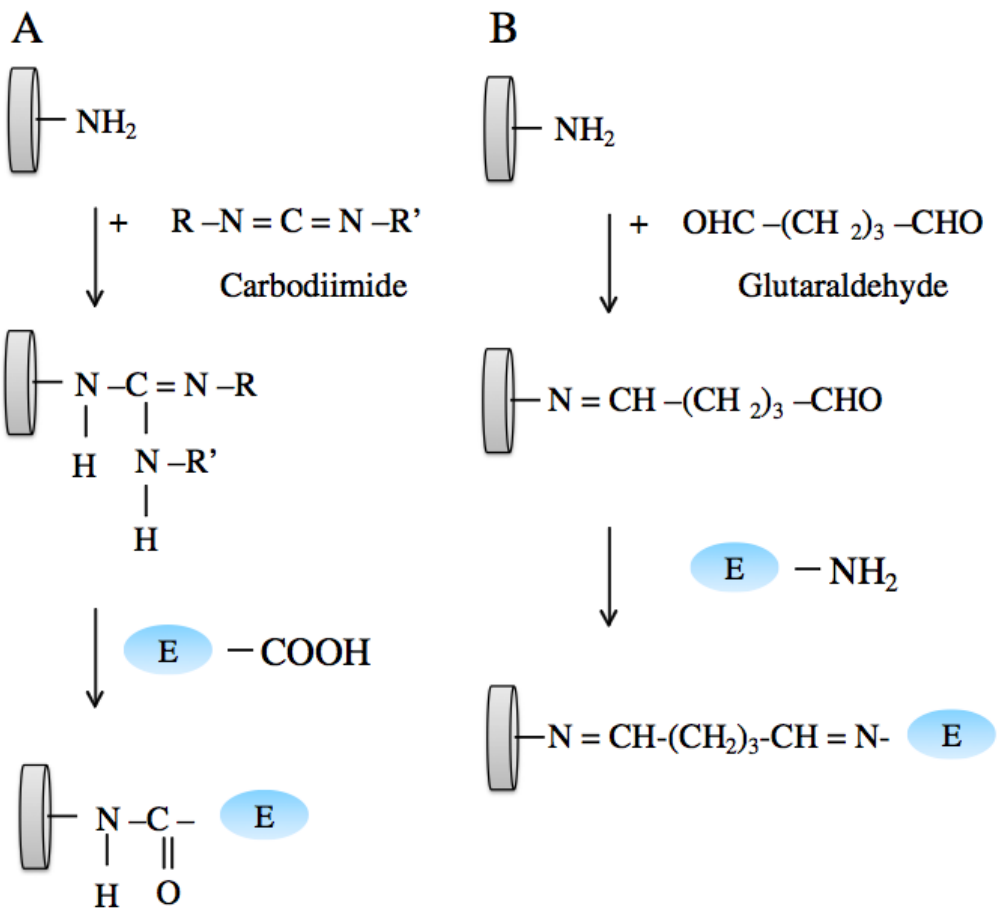

Figure 1.9 Reaction Scheme for Carbodiimide or Glutaraldehyde
Immobilization reaction scheme with A) Carbodiimide or B) glutaraldehyde (Adapted from *Biotechnol. Adv.* **30,** 489–511 (2012))

To avoid some of the negative aspects of non-specific crosslinking reagents, researchers have begun using methods that result in single unique attachment of enzymes to functionalized supports. A good example is an enzyme with an exposed thiol group that can be bound directly to gold surfaces. Reagents can be used to convert other functional groups to thiol groups or site-directed mutagenesis can be used to introduce cysteine residues. Park and co-workers[27] successfully immobilized protein G, an antibody binding protein, on gold surfaces through a cysteine residue engineered on the N-terminus of the protein. Liu et al. used site directed mutagenesis to introduce cysteine residues in pyrophosphatase to successfully bind the enzyme to gold nanoparticles[28]. Their experiments were directed towards measuring the effect of surface density on gold nanoparticles and the resulting changes in enzyme activity.

Another route for directed covalent immobilization is the use of self-assembling monolayers (SAMs). A common approach to preparing SAMs involves decorating surfaces with carboxylic acid or amine functional groups. Biomolecules can then be coupled to the SAM surface with coupling reagents such as carbodiimide or glutaraldehyde. Using a similar method Cabrita and coworkers successfully made N-hydroxysuccinimide ester terminated SAMs on gold surfaces to bind laccase through amine groups on the enzyme[29].

A valuable reaction for binding biomolecules to a surface through a single, defined anchor point is the reaction of thiols with maleimide. A diagram of this type of immobilization is shown in Figure 1.10. This chemistry lends itself particularly

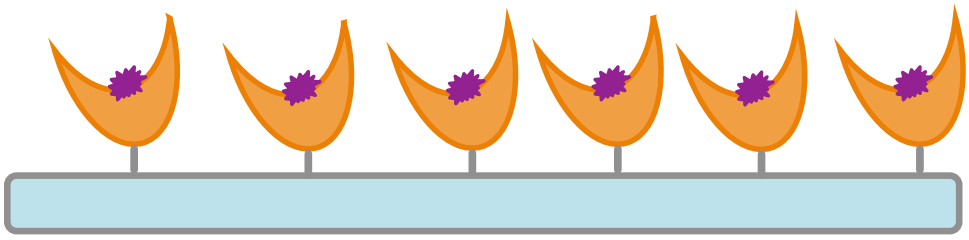

Figure 1.10 Diagram of Specific Covalent Enzyme Immobilization
Diagram of specific enzyme immobilization. Enzyme represented in orange, active site represented in purple.

well for use on enzymes for a number of reasons. Cysteine residues do not often occur naturally on the surface of proteins, making site-directed mutagenesis ideal for placing cysteine residues in discrete locations for site-specific attachment. Thiols are more reactive relative to other chemical groups present on the surface of the enzyme and the Michael addition to maleimide is specific and irreversible reaction[30]. Maleimide is stable and can be derivatized under biological conditions, which makes it compatible with the immobilization of biological molecules in aqueous environments[31].

While much work has been done to establish methods for immobilization, the field of enzyme immobilization lacks a molecular level understanding of the relationship between enzyme surface orientation, catalytic activity, and enzyme stability. A decrease in specific activity upon enzyme immobilization has frequently been reported[18,32–34], and whereas various hypotheses for this decrease have been put forward, very few rigorous studies have been undertaken to substantiate them.

Among these hypotheses are that the diffusion of substrate to the immobilized enzyme and/or product to/away from the immobilized enzyme could limit activity as compared to enzyme in free solution. Another explanation is that electrostatic interactions between the immobilized enzyme and the surface could distort the enzyme structure or active site and reduce activity. Changes in protein tertiary structure also play a role in activity changes[33]. For example immobilized lipases show an increase in specific activity hypothesized to be caused by the permanent opening of a lid that covers the active site. Activity can be reduced for similar changes in structure.

The change in stability of immobilized enzymes is another important parameter that is poorly understood. There are many reports of increased stability for immobilized enzymes, which is generally attributed to reduced enzyme mobility that prevents unfolding or a reduction in aggregation. It has been proposed that immobilization increases stability towards unfolding by organic solvents by reducing exposure to bulk solution. However, in some cases immobilized enzymes can exhibit a decrease in stability[35].

Researchers have turned to molecular dynamics simulations to describe the underlying mechanisms that drive the behavior of immobilized enzymes. For example, Wei and Knotts created an improved course-grained model for simulating immobilized enzymes and their interactions with surfaces[36]. The proteins in this case were modeled with each amino acid residue being represented by a bead, instead of an atomistic model where each atom is represented. The modeled

structure was stabilized by defining the hydrogen bonds that exist based on the crystal structure. A single residue attachment was modeled on three different surfaces: hydrophobic, mildly hydrophobic and hydrophilic. It was found that the greatest number of native contacts remained intact when the protein was immobilized on the hydrophilic surface. In contrast, the modeled protein unfolded onto the hydrophobic surface. The authors showed that on a hydrophilic surface a larger energy barrier helps keep the protein away from the surface and maintain its native contacts.

A course-grained model was employed by Moskovitz and Srebnik for use on globular proteins[37]. The authors simulated the adsorption of lysozyme on a hydrophobic surface to study the changes in the proteins structure. They observed a 35-75% decrease in energy due to absorption relative to folded enzyme free in solution. The authors suggest that the amount of energy decrease depends on the conformational stiffness of the native structure of the protein being adsorbed. When the lysozyme model was simulated as adsorbed the α-helices spread out due to the hydrophobic residues being attracted to the surface and the β-sheets completely lost their structure. The authors propose that this is due to the more hydrophobic nature of β-sheets as compared to α-helices and proposed that these types of models can be used to predict an adsorbed protein's functional properties.

The effects of multiple tether sites on an immobilized enzyme was explored through modeling by Loong and Knotts[38]. The authors hypothesized that multiple tethers would lend more stability to the protein than instances where only one

tether is used. The data from their simulations showed that using two tethers significantly increased the stability of the native folded state by removing unfolded intermediates. A caveat to this gained stability is activity. In some cases while stability of the immobilized enzyme is preserved activity is still lost. While a lot has been achieved in the realm of molecular dynamics simulations, there is very little empirical evidence to test these hypotheses.

1.4 Goals of this Work

The crux of this research was to build a more complete picture of the interplay between activity, stability, orientation, and surface characteristics for immobilized enzymes. To reach this goal, we used Nitroreductase B (NfsB) as a model enzyme. To achieve a uniform, directed, and intentionally oriented configuration of the enzyme with respect to the surface, the use of a single chemically defined covalent surface-attachment method was used. Silane self-assembling monolayers (SAMs) formed from maleimide-terminated polyethylene glycol (PEG) linkers were employed to crosslink to surface cysteine residues engineered onto the surface of NfsB. Different chemical functional groups were displayed on the SAM surface to observe the effects of changes in surface characteristics on enzyme activity and stability. The catalytic activity and stability of the immobilized enzyme was assessed for several different orientations of the enzyme with respect to the surface and different SAM surface functional groups. In collaboration with the laboratory of Dr. Zhan Chen, sum frequency generation (SFG)

vibrational spectroscopy, a surface specific technique, was used to gain valuable insight on the orientation of immobilized NfsB.

Chapter two describes the development of NfsB as our model enzyme. Two NfsB constructs were created, each containing a unique, solvent-exposed cysteine residue in different loops of the protein. These cysteine residues were used to covalently bind NfsB to the maleimide-functionalized SAM surface. Kinetic parameters for NfsB in solution were measured and used to determine that the surface cysteine residues did not have an effect on activity of the enzyme. We developed an activity assay for immobilized NfsB samples and establish the micro-bicinchoninic acid assay as an accurate way to quantify immobilized enzyme. SFG was used to determine, experimentally, the immobilized enzyme orientation.

Chapter three describes experiments aimed at examining the thermal stability of immobilized enzyme. We created mixed functionality SAM surfaces by functionalizing the glass surface with alcohol and methyl terminated PEG linkers in addition to the maleimide-terminated linkers. By changing the characteristics of the SAM surface we explored its effects on the activity and stability of immobilized NfsB. In addition to the two previously described NfsB constructs that had anchoring cysteine sites located on loops, we created a third construct which positioned the cysteine on an α-helix. We measured the effects of loop versus helix anchor point attachment on the activity and stability of the immobilized enzyme.

In Chapter four we consider the definition of a monolayer and explored the parameter of surface density. The surface density was modulated to measure the

effects on activity and stability of immobilized enzyme for all three NfsB constructs. Higher molecular weight PEG linkers were co-immobilized along with NfsB to determine if there was any additional thermal stability provided. Chapter five presents all the details on the materials and methods used for these experiments. The final Chapter six discusses the meaning and implications of all the results and future directions.

Chapter 2

Determining Effect of Immobilization Orientation on Activity of NfsB

2.1 Introduction

The loss of catalytic activity upon enzyme immobilization has been reported extensively in the literature[39,34]. There are many hypotheses as to why. For example, in a system where enzymes are embedded in a solid support, diffusion of substrates and products could be limiting as compared to enzyme in solution[25]. In a physically adsorbed system, strong interactions between the surface and the enzyme could cause partial unfolding of the enzyme on the surface and reduce activity that way[2].

In this chapter we consider the effects of orientation on enzyme activity. When immobilizing an enzyme, retention of the highest catalytic activity is an important goal. This work was done to make a clearer picture of the behavior of a protein when it binds a surface in regards to orientation, or position of the active site relative to the surface and its relationship to retained catalytic activity. If an active site is occluded, this could be a contributing factor to a reduction in activity. Perhaps, one orientation would lead to unfavorable protein-surface interactions that reduce activity but not another orientation. We wanted to learn whether or not the orientation of the immobilized enzyme has an affect on the activity or the

stability of the enzyme. To begin to answer these questions, experimentally, we need a surface to uniformly attach enzyme, a model enzyme and a way to assess orientation and activity.

To control the orientation of the enzyme, we used maleimide-functionalized silane self assembling monolayers (SAMs) on glass surfaces that are reactive towards exposed cysteine residues[40]. Thiol-reactive maleimide chemistry is ideal for enzyme immobilization, because cysteine residues do not occur frequently on the surface of proteins in Nature[30]. This allows us to use site directed mutagenesis to place cysteine residues in specific locations on the protein surface that serve as points for attachment to the abiologic surface. Thiols are very reactive relative to other groups present on protein surfaces, so the Michael addition to maleimide is a selective and robust process. Finally, maleimide is stable under biological conditions making the immobilization of enzyme in aqueous solution possible.

SAMs provide a good model surface for our studies because they are atomically flat and chemically defined. The linkers that make up the SAM surface comprise a silane group that is reactive toward glass, a short ethylene glycol (EG) chain that acts as a spacer and are terminated with a maleimide group (Figure 2.1). EG chains reduce the possibility of unfavorable protein-linker interactions or non-specific adsorption of protein onto the surface. The maleimide moiety of the linker

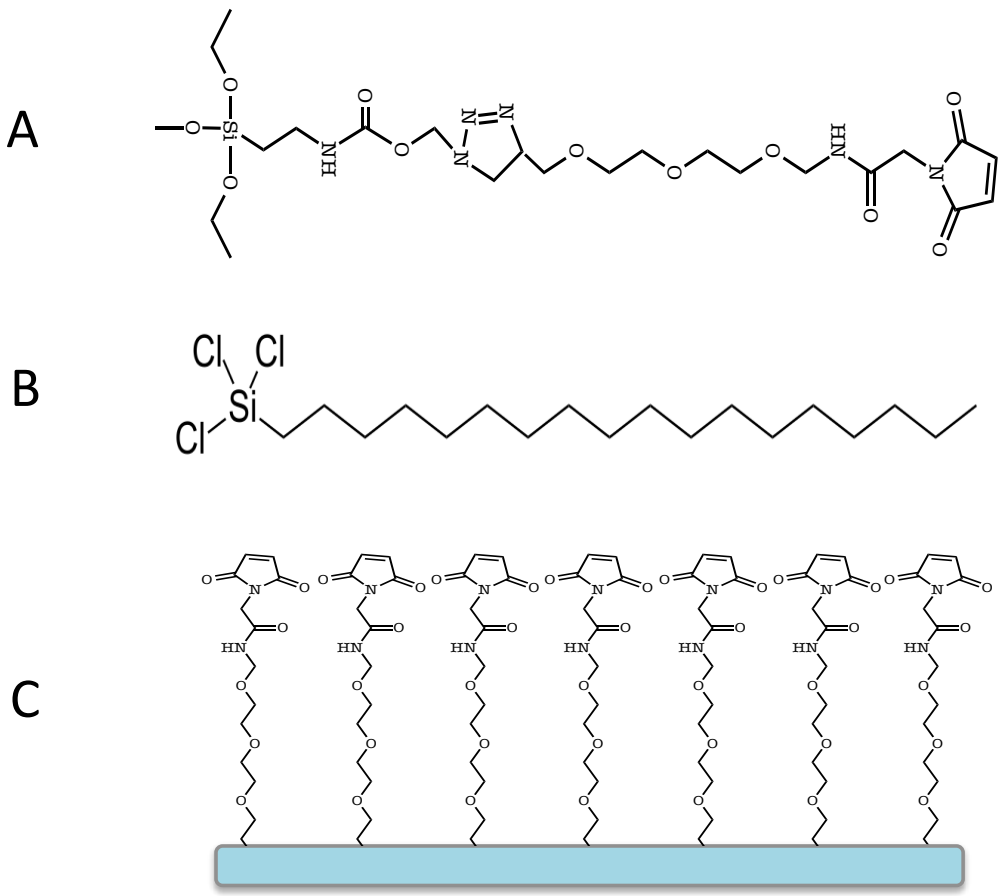

Figure 2.1. Structures of EG_3-Maleimide Linker, OTS and Diagram of Maleimide Functionalized SAM Surface

A) EG_3-maleimide linker: silane with EG chain spacer terminated with maleimide group, B) Octadecyltrichlorosilane C) Diagram of maleimide functionalized glass surface

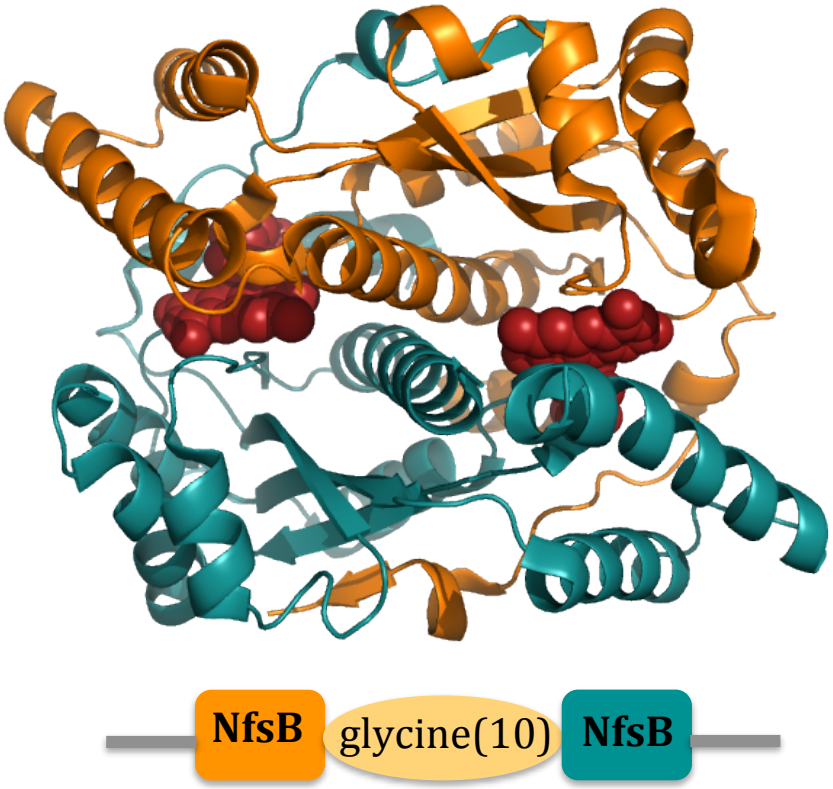

Figure 2.2. NfsB Structure and Diagram of Gene
Top) NfsB structure with FMN cofactor shown in red
Bottom) Diagram of fusion gene

reacts covalently with the surface cysteine residue engineered on the protein surface. As a comparison for non-specific adsorption, we used a SAM surface comprising octadecyltrichlorosilane (OTS) which is hydrophobic and provides a surface for non-specific adsorption.

Nitroreductase B (NfsB) is the model enzyme employed in these studies (Figure 2.2). NfsB belongs to a family of flavin-containing nitroreductases, which catalyze the reduction of quinones and aromatic nitro-groups among other substrates[41]. NfsB uses nicotinamide adenine dinucleotide (NADH)[42] as an electron donor and in our studies 4-nitrobenzenesulfonamide serves as a convenient substrate. Catalytic activity is measured by following NADH oxidation at 350 nm. Much is already known about NsfB, making it a good model enzyme. The structure has been solved (PDB 1DS7)[43], which allows us to systematically select surface residues available for immobilization sites. NfsB is natively expressed as a homo-dimer, so to be able to insert single surface cysteine residues by site directed mutagenesis, a codon-optimized fusion protein was designed that connects the two monomers with a ten-residue glycine linker. Native NfsB has a pair of active sites situated at the interface of the two monomers with flavin mononucleotide prosthetic groups in the active sites. The *NfsB* fusion gene was commercially synthesized and cloned in the pET28b bacterial expression vector.

The experiments described in this chapter utilize two NfsB constructs designed to orient the protein along roughly orthogonal axes. NfsB V424C places a

cysteine residue on a loop adjacent to one active site. This orients the active sites, upon immobilization, perpendicular to the SAM surface with one active site facing the bound surface and the other active site exposed to solution (Figure 2.3). NfsB H360C places the cysteine on another loop distal to the active sites orienting the active sites parallel to the surface. Both construct structures are shown in Figure 2.3. For control purposes a construct lacking a surface cysteine was also created.

A major challenge in the field of surface-immobilized enzyme is obtaining information about the secondary structure and orientation[44]. This is because traditional techniques to assess protein structure (x-ray crystallography, NMR, etc.) are unsuitable for proteins covalently bound to a solid support. Structural information regarding the orientation of the enzyme bound to the EG-maleimide SAM surface was obtained using sum frequency generation through collaboration with the laboratory of Professor Zhan Chen.

Sum frequency generation vibrational spectroscopy (SFG) is a second-order nonlinear optical technique that occurs in non-centrosymmetric media such as surfaces and interfaces[45]. In the SFG setup, two laser beams are overlapped spatially and temporally with each other on an SFG-active sample, like a surface with protein immobilized. One beam is 532 nm visible laser and the other is a tunable IR beam whose range covers the vibrational frequencies of interest, in this case the amide stretch of proteins. SFG signals will be resonantly enhanced when the frequency of the tunable IR beam matches an SFG sensitive vibrational transition, amide modes

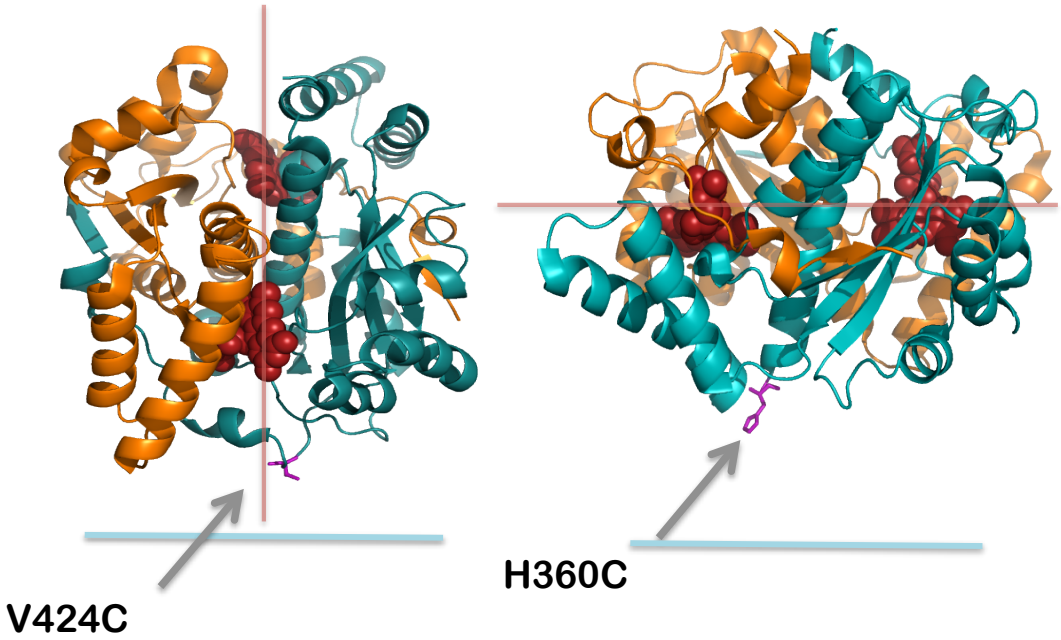

Figure 2.3. Structure and Orientation Diagram of NfsB Variants
Intended orientation of two NfsB construct structures, V424C (left) and H360C (right). The functionalized glass surface represented in blue, symmetry axis running through active sites highlighted by red line.

of proteins. Therefore, as the IR is tuned to the amide stretch, a photon will be produced whose frequency is the sum of the frequencies of the two input photons[46]. Two SFG spectra are taken using different polarizations, ssp (s-polarized SFG signal, s-polarized visible beam, and p-polarized IR beam) and ppp. The two polarizations probe the orientation of the α-helices in the protein structure. The measured ratio of the effective second-order nonlinear optical susceptibility tensor components detected from these two spectra is used to calculate the orientation of the α-helix in the protein molecule. SFG is a very useful tool for analyzing the structure of surface immobilized proteins and gave us insight into the orientation of our immobilized proteins.

2.2 Results

2.2.1 NfsB in Solution

NfsB is utilized as our model enzyme to study the effects of attachment orientation on activity. Wild type NsfB is expressed with one cysteine and as a homodimer. For our experiments, a fusion protein was designed and the gene was commercially synthesized with one cysteine in position 424. The native cysteine at position 85 was changed to an alanine residue (sequence provided in the Materials and Methods Chapter 5.1). A cysteine-free construct and a construct with a cysteine at position 360 were constructed by site-directed mutagenesis. *E. coli* BL21(DE3) cells were transformed with these NfsB expression vectors and expressed in 2XYT mediat at 37 °C until reaching an OD of 0.6 at 600 nm at which point they were induced with the additions of IPTG (1mM). Cultures were then grown overnight at

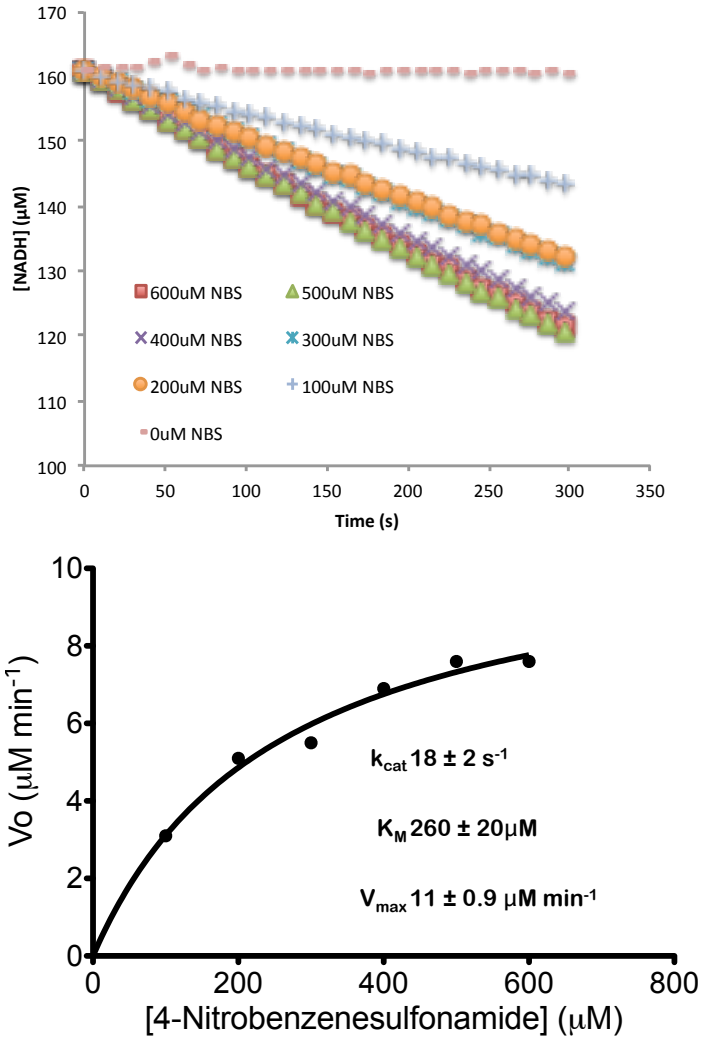

Figure 2.4. Catalytic Activity of NfsB in Solution
NADH concentration versus time for NfsB in solution (top). Michaelis Menten curve for NfsB in solution (bottom).

18 °C and harvested by centrifugation. Full expression and purification methods listed in the Materials and Methods Chapter section 5.2 and

5.3. All three constructs expressed well, typically yielding around 80 mg enzyme per liter of culture. Purification was performed utilizing a 6-histidine tag and nickel affinity chromatography yielding proteins of greater than 90% purity. The availability of surface cysteine residues present on the purified proteins were quantified using Ellman's reagent (Materials and Methods Chapter section 5.5) and confirmed to be present in stoichiometric quantities.

NfsB-V424C and NfsB-H360C both situate the surface cysteine sites located on loop regions of the secondary structure of the protein. These were chosen to avoid affecting the folding or activity of the protein. These two sites were also designed to lead to two orthogonal orientations.

Steady-state kinetic parameters were measured for these variants in solution. All catalytic activity assays were performed in PBS with 160 μM NADH and 4-nitrobenzenesulfonamide in varying concentrations. The detailed methods are outlined in the Materials and Methods Chapter section 5.11. A representative Michaelis Menten curve is shown in Figure 2.4. The activity compared to wild type indicate that the cysteine mutations do not affect folding or activity of the enzyme. Specific activity was measured in PBS at ambient temperature with 160 μM NADH and 500 μM 4-nitrobenzenesulfonamide (Materials and Methods Section 5.11). Specific activities were measured in solution for NfsB-V424C, NfsB-H360C and NfsB-C85A and are shown in Table 2.1.

Table 2.1 Specific activity of three NfsB variants in solution

NfsB Variant	Specific Activity (µmol/min/µg NfsB)
V424C	24 ±1.0
H360C	27 ±1.6
C85A	20 ±0.8

2.2.2 NfsB Bound to Surface

A major technical challenge to characterizing immobilized proteins has been measuring surface concentration. Traditional concentration measurements such as UV absorption, Bradford assay or Lowry assay are unsuitable for surface bound protein because the measurements require the protein to be in solution. In our studies we have applied the bicinchoninic acid assay (BCA). BCA is amenable to surface bound protein because the chromophore (copper BCA complex), which is measured spectroscopically by absorbance at 562 nm, is dissociated from the protein and released into solution (Figure 2.5). The accuracy of the BCA protein quantification was confirmed by amino acid analysis.

Initially, NfsB-H360C and NfsB-V424C were immobilized on beads functionalized with maleimide-EG_4-silane (Nanocs, USA). This linker was bound directly to acid washed glass beads in anhydrous toluene, with gentle agitation

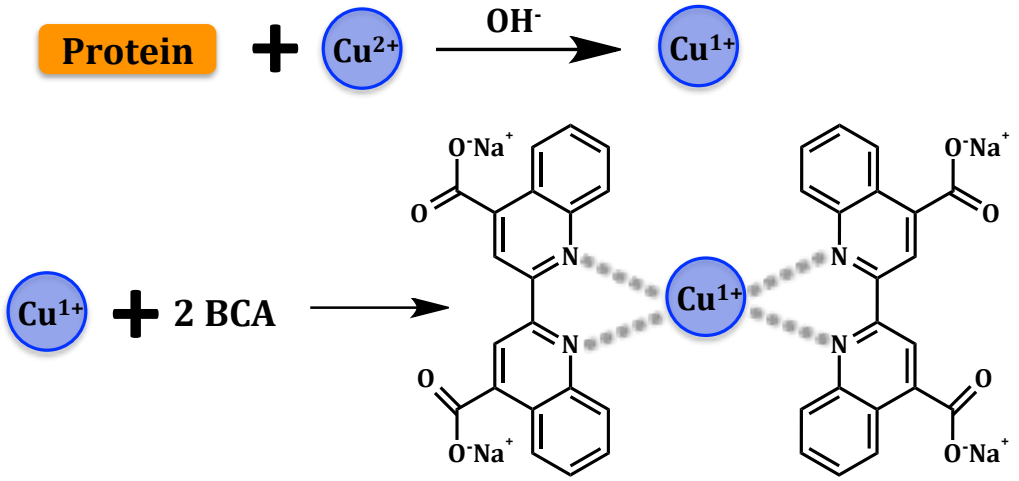

Method	Protein (ng mg-glass^{-1})
Amino Acid Analysis	53 (±3)
BCA	68 (±5)

Figure 2.5. Determintation of Surface Protein Concnetration
Diagram of BCA reaction mechanism (top). Amino acid analysis result compared to BCA result for concentration measurement (bottom).

overnight. Beads were then washed with toluene 3 times, followed by 3 washes with DMSO followed by 3 washes with PBS buffer. Enzyme (5 μM) was immobilized to bead samples in PBS buffer at 4 °C with gentle agitation overnight. Beads were washed with PBS to eliminate unbound enzyme. Activity of immobilized enzyme was measured by UV absorbance at 340 nm. The functionalized beads were suspended in the reaction mixture (160 μM NADH, 300 μM ferricyanide, in PBS) and the UV absorbance was measured every 30 seconds for two minutes. NfsB-H360C had a specific activity of 14±1 μM/min/μg enzyme and NfsB-V424C had a specific activity of 7±2 μM/min/μg enzyme[47]. After these initial experiments, the maleimide-EG_4-silane reagent became unavailable which necessitated a complete change in SAM surface functionalization reagents to the click-chemistry system with EG_3-maleimide described below.

Activity assays on immobilized NfsB were performed with NfsB immobilized on 75 μm diameter glass beads (Materials and Methods Chapter section 5.7). Glass beads were activated with piranha solution overnight followed by rinsing with copious amounts of DI water until neutral pH was achieved. The beads were then rinsed with DMSO followed by toluene. The beads were then silanized with silane-alkyne (0.1%) in anhydrous toluene overnight. Unbound silane-alkyne was rinsed away with toluene and then DMSO. Azido-EG_3-maleimide was bound to alkyne functionalized surface in a click reaction with 1 mM copper sulfate and 50 mg mL^{-1} sodium ascorbate in 50% DMSO in DI water. The reaction was incubated overnight at room temperature. The beads were then thoroughly washed with water and incubated with EDTA to remove any excess copper. Finally, the beads were washed

again with buffer before being incubated with enzyme solution (5 μM, PBS) at 4 °C overnight. Excess enzyme was washed away with a 5% solution of Tween-20 followed by washing with more PBS buffer. Activity measurements were made on freshly prepared immobilized enzyme samples.

Attaching the enzyme to beads increases the surface area available for enzyme binding and thereby increases the protein concentration in the reaction. The BCA reaction was used to measure surface coverage of bound enzyme on the bead surface. Enzyme bead samples were incubated with the BCA reaction mixture (Materials and Methods Chapter section 5.9) at 60 °C for 15 minutes before being cooled to room temperature. The samples were mixed by vortex and the absorbance at 562 nm was measured. A prepared standard curve was referenced for concentration calculations. NfsB-V424C and NfsB-H360C were found to bind at 87±5 ng per mg of beads, consistent with a monolayer of coverage which is less than or equal to 106 ng enzyme per mg of beads based on 4 enzymes per 10,000 $Å^2$ surface area. OTS beads with physically adsorbed enzyme results in surface coverage of 500±42 ng/mg beads, which is a significantly higher concentration than what would be consistent with a monolayer.

Activity was measured for NfsB covalently bound to EG_3-maleimide functionalized beads and NfsB physically adsorbed to OTS functionalized beads (Materials and Methods Chapter section 5.12 and above). The activity of immobilized enzyme was followed by UV absorbance at 340 nm. The functionalized beads were suspended in the reaction mixture (160 μM NADH, 500 μM 4-

nitrobenzenesulfonamide, in PBS) and the UV absorbance was measured every 30 seconds for two minutes. The results are shown in Figure 2.6. The specific activity for NfsB bound to maleimide functionalized beads was found to be 5.8±0.5 μM/min/μg enzyme whereas the specific activity for NfsB physically adsorbed to OTS functionalized beads was found to be 1.4±0.2 μM/min/μg enzyme. The loss of activity on the OTS surface can likely be attributed to partial unfolding of the enzyme or unfavorable orientations due to the non-specific nature of the immobilization.

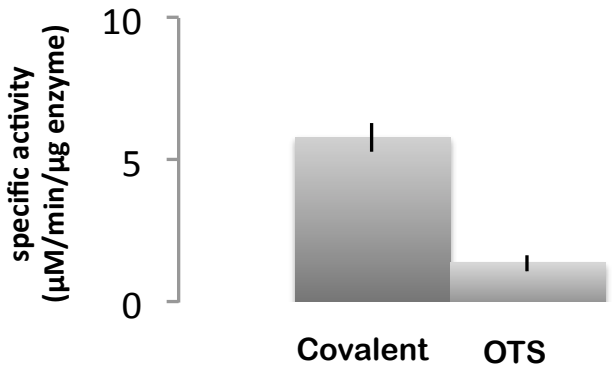

Figure 2.6. Specific Activity for Immobilized NfsB
NfsB-V424C specific activity covalently immobilized through EG_3-maleimide linker and non-specifically adsorbed through OTS functionalized glass beads

Through collaboration with the Chen lab SFG and attenuated total reflectance-Fourier transformation infrared spectroscopy (ATR-FTIR) were used to obtain information on the orientation of bound enzyme. Initial SFG spectra (shown in Figure 2.7) were used to validate our approach by showing that the amide I peak, around 1655 cm^{-1} is present only after NfsB is bound to the PEG-maleimide SAM surface and remains after washing. SFG and attenuated total reflectance-Fourier

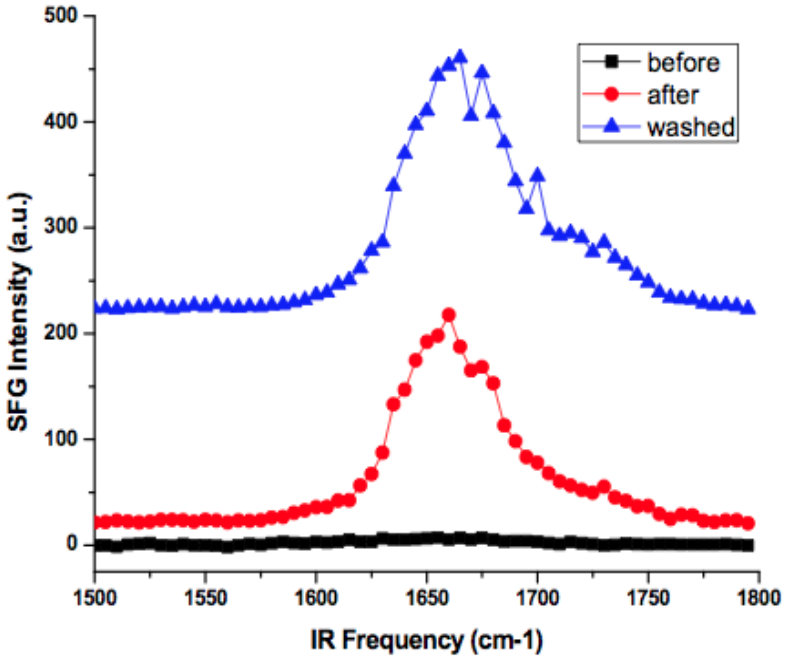

Figure 2.7. SFG Spectra
SFG specra taken before protein binding (black), before washing (blue- offset) and after washing (red) showing confirmation of enzyme binding. Spectra taken and analyzed by Dr. Lei Shen.

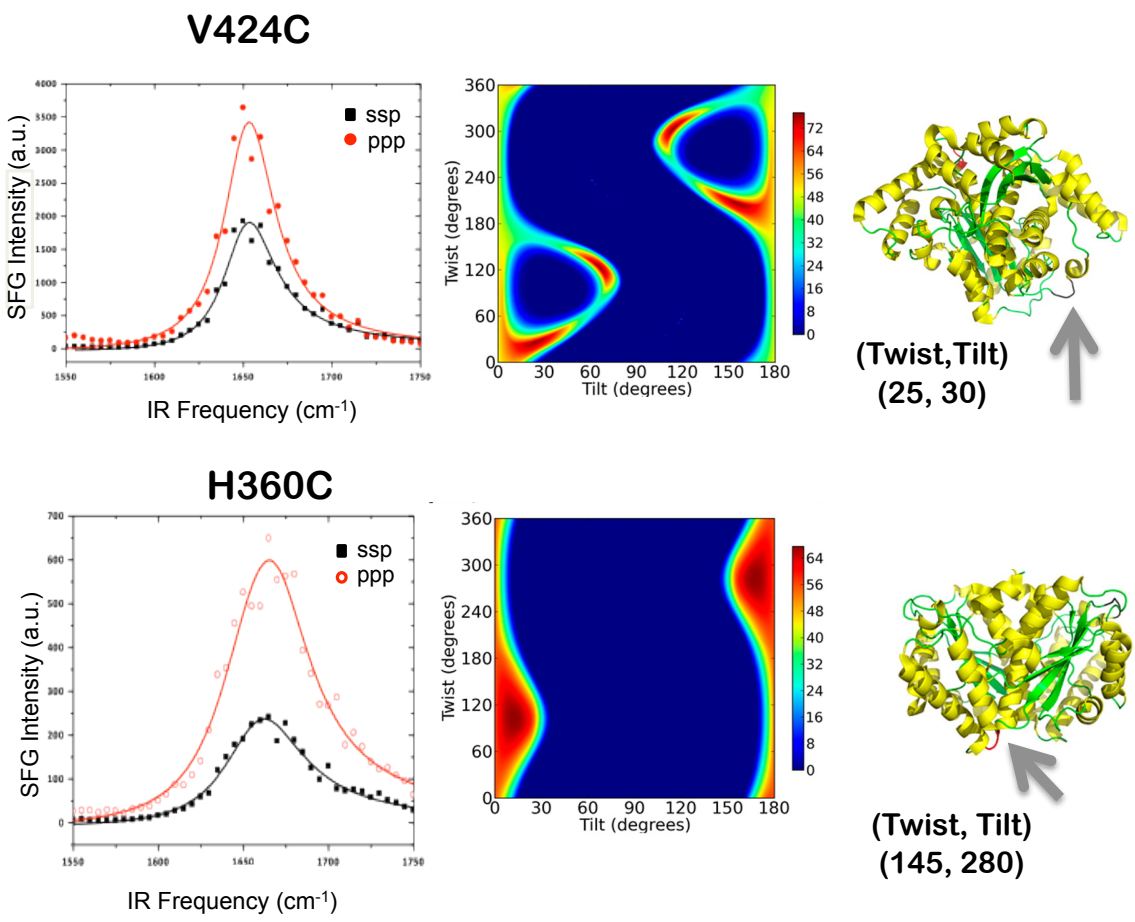

Figure 2.8. SFG spectra and resulting heat maps for twist and tilt angles. Structures showing measured orientation (right). Spectra taken and analyzed by Dr. Lei Shen

transformation infrared spectroscopy (ATR-FTIR) were used to determine the orientation of immobilized enzyme on maleimide SAM surfaces. The results are shown in Figure 2.8.

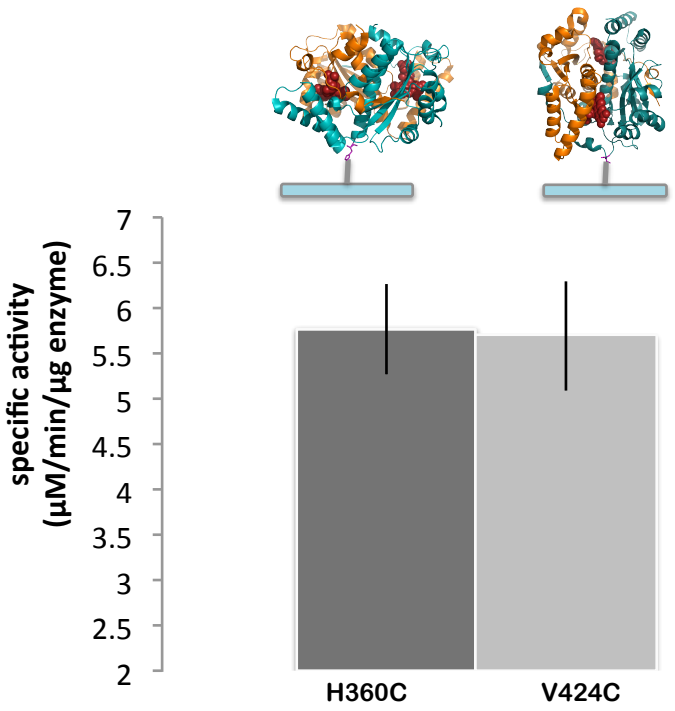

Figure 2.9. Specific Activity of Immobilized NfsB
Specific activity of two orientations of NfsB H360C and V424C, structure diagrams indicating orientation shown above

The activities of NfsB H360C and NfsB V424C were measured when bound to EG_3-maleimide functionalized SAM beads. The results are shown in Figure 2.9. NfsB-H360C orients the active sites parallel to the SAM surface, so each active site is equally exposed to bulk solution. NfsB-V424C orients the active sites perpendicular to the bead surface with one active site facing out into bulk solution and one active site facing the bead surface. The specific activities for these two opposing

orientations were measured as 5.8±0.5 μM/min/μg enzyme for the H360C construct and 5.7±0.6 μM/min/μg enzyme for the V424C construct. These two values are the same within error. This shows that the orientation of immobilized NfsB does not change the specific activity on the EG_3-maleimide SAM surface.

2.3 Discussion

The field of immobilized enzymes currently lacks a comprehensive understanding of the loss of activity upon immobilization. The work described in this chapter was performed to gain some insight on the relationship between the orientation of immobilized enzyme and specific activity. We started by making uniform, chemically defined SAM surfaces functionalized with maleimide as a surface to bind NfsB through single cysteine residues. The protein concentration for immobilized samples was measured using the BCA reaction and the accuracy of the reaction was confirmed by amino acid analysis.

An activity assay for immobilized NfsB was developed based on UV absorbance using NADH and 4-nitrobenzenesulfonamide as a substrate. This activity assay was used to measure the specific activity for NfsB bound to a maleimide functionalized SAM surface and OTS. The physically adsorbed OTS surface resulted in a specific activity that was 4 times less than the enzyme tethered on the maleimide SAM surface. This supports the idea that the physically adsorbed enzyme may be immobilized in unfavorable orientations or be partially unfolded,

therefore resulting in a drastically lower specific activity.

Two NfsB constructs were used in these experiments, H360C and V424C. We hypothesized that placing the cysteine residue in position 360 would result in the enzyme being oriented such that the active sites would be equally exposed to solution and be approximately parallel to the bound surface (Figure 2.3). We also hypothesized that the cysteine residue in position 424 would result in the enzyme being oriented such that one active site would be facing toward the binding surface and the other active site would be out in bulk solution (Figure 2.3). The SFG and ATR-FTIR results confirm these expected orientations, shown in Figure 2.8.

It is important to note here, the difference in activity measurements for the silane-EG_4-maleimide functionalized surface, which did show a difference in specific activity for the two orientations. This highlights the importance of the role that the surface plays in the activity of immobilized enzyme. It also shows a potential substrate effect, as ferricyanide was the substrate used on the silane-EG_4-maleimide immobilized enzyme and 4-nitrobenezenesulfonamide was the substrate utilized in the reactions with EG_3-maleimide immobilized enzyme. The specific activity was higher with ferricyanide than 4-nitrobenzensulfonamide. Further experiments using ferricyanide as a substrate on EG_3-maleimide immobilized enzyme are necessary to determine if this was a surface effect or a substrate effect.

We measured the specific activity for NfsB-H360C and NfsB-V424C immobilized on an EG_3-maleimide functionalized surface and found them to have the same specific activity. This suggests that orientation of immobilized enzyme

didn't have an effect on activity in these experiments, although its clear that specifically oriented covalent immobilization provides a significant increase in specific activity compared to non-specific physical adsorption.

Chapter 3

Effects of Attachment Site and Surface Composition on Immobilized NfsB Activity and Stability

3.1 Introduction

An important feature of immobilization is its impact on the stability of the enzyme. The stability is an important criterion that affects the ability to reuse, store, and optimize reaction temperatures[9,48]. In previous studies, it has been found that immobilization can have a stabilizing effect on proteins under certain conditions[10,49,17]. The reason for the often-observed stabilization is poorly understood but could be attributed to the free energy of unfolding. The reduction of degrees of freedom imposed by the presence of the abiotic immobilization surface decreases the entropy and thereby increases the free energy necessary for unfolding. Another important thing about stability is that researchers use a variety of different ways to assess stability. A common way is to use chemical denaturants or heat[50]. Some studies use mechanical forces or biological denaturants like proteases[50]. In our studies, we used a temperature-based assay to measure stability. Here, we aim to gain a better understanding of the influence the surface has on immobilized enzyme stability/activity and the effect of surface cysteine placement on immobilized enzyme stability.

3.1.1 Mixed Surfaces

In this chapter we explore the effects of the abiotic surface properties on immobilized enzyme stability and activity by varying the functional groups present on the surface. Using the covalent attachment to glass via maleimide-EG_3 linker established in Chapter 2, these experiments were performed to determine how changes to the maleimide-SAM surface affects the activity and stability of covalently tethered enzymes. The SAM surface prepared for these studies utilized methyl-terminated (EG_3-ME) and alcohol-terminated (EG_3-OH) EG linkers (Figure 3.1) in addition to maleimide-terminated (EG_3-MAL) EG linkers. SAM surfaces were

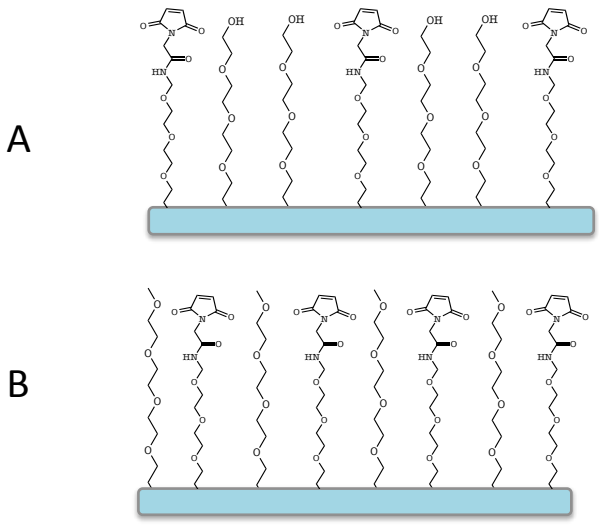

Figure 3.1. Surfaces Studied in this Chapter
A) Diagram of mixed EG_3-maleimide and EG_3-OH terminated SAM on glass, B) Diagram of mixed EG_3-maleimide and EG_3-methyl terminated SAM on glass

prepared on 75 μm diameter glass beads (Materials and Methods Chapter section 5.7). The glass beads were silanized in anhydrous toluene with silane-alkyne (0.1%) overnight with gentle agitation. Excess silane-alkyne was washed away with toluene

followed by DMSO. PEG linkers were attached to the alkyne-functionalized beads in a click-reaction. Three types of SAM surfaces were prepared for these experiments: 1:1 mole ratio, 1:10 mole ratio, and 1:20 mole ratio surfaces. For the 1:1 mole ratio the SAM surfaces were functionalized with a 1:1 mole ratio of EG_3-MAL:EG_3-OH or EG_3-MAL:EG_3-ME. The 1:10 mole ratio surfaces were functionalized with a 1:10 mole ratio of EG_3-MAL:EG_3-OH or EG_3-MAL:EG_3-ME. The 1:20 mole ratio surfaces were functionalized with a 1:2 mole ratio of EG_3-MAL:EG_3-OH or EG_3-MAL:EG_3-ME. We measured the specific activity of NfsB-V424C and NfsB-H360C immobilized on each of these prepared SAM surfaces.

3.1.2 Stability

The thermal stability of immobilized NfsB on mixed-functionality SAM surfaces with varying hydrophobic properties are explored in this chapter. First we assessed the stability of NfsB in solution. These assays were performed by heating the enzyme sample for 5 minutes to a temperature between 20 °C and 65 °C. To prevent loss from the active sites, FMN was added to these assays as described in the Materials and Methods Chapter section 5.13. After heating, the sample was brought to room temperature for 10 minutes, followed by measurement of the remaining specific activity (Materials and Methods Chapter 5.13). The fraction of remaining activity was plotted as a function of temperature and these curves were fit to calculate T ½, the temperature at which half the specific activity remains. The T ½ values were used as a comparison of thermal stability.

For the immobilized enzyme experiments we prepared a set of SAM surfaces (Materials and Methods Chapter section 5.7) functionalized with a total of 12 nmol linker per g of beads. The surface concentration of EG_3-MAL was held constant at 1.2 nmol/g beads. The remaining 10.8 nmol/g beads was made up of a range of mixtures of EG_3-OH and EG_3-ME to produce a range of hydrophobicity. In total, 6 types of SAM surfaces were prepared: 100%-EG_3-ME, 90%-EG_3-ME 10%-EG_3-OH, 75%-EG_3-ME 25%-EG_3-OH, 25%-EG_3-ME 75%-EG_3-OH, 10%-EG_3-ME 90%-EG_3-OH, and 100%-EG_3-OH. This means the most hydrophobic surface was the 100%-EG_3-ME and the most hydrophilic surface was the 100%-EG_3-OH and there were 4 gradations in between. NfsB-H360C and NfsB-V424C were immobilized to each of these SAM surfaces and the specific activities and T ½ values were measured. Comparing T ½ and specific activity values from solution and for enzymes immobilized on different SAM surfaces provides insight into the stabilizing effects of immobilization and the effects of the hydrophobicity of the SAM surfaces tested.

3.1.3 Loop vs Helix

Finally, we examined an NfsB construct with an anchoring cysteine residue placed on a rigid α-helix to determine effects of attachment point on stability compared to anchoring residues on loop regions. Immobilized enzymes are used in a variety of applications as discussed in the introduction[10,49,51,52]. Often these enzymes are non-specifically immobilized which might have a negative impact on catalytic activity. However, an understanding of the relationship between attachment site and its impact on enzyme stability and activity is largely lacking. In

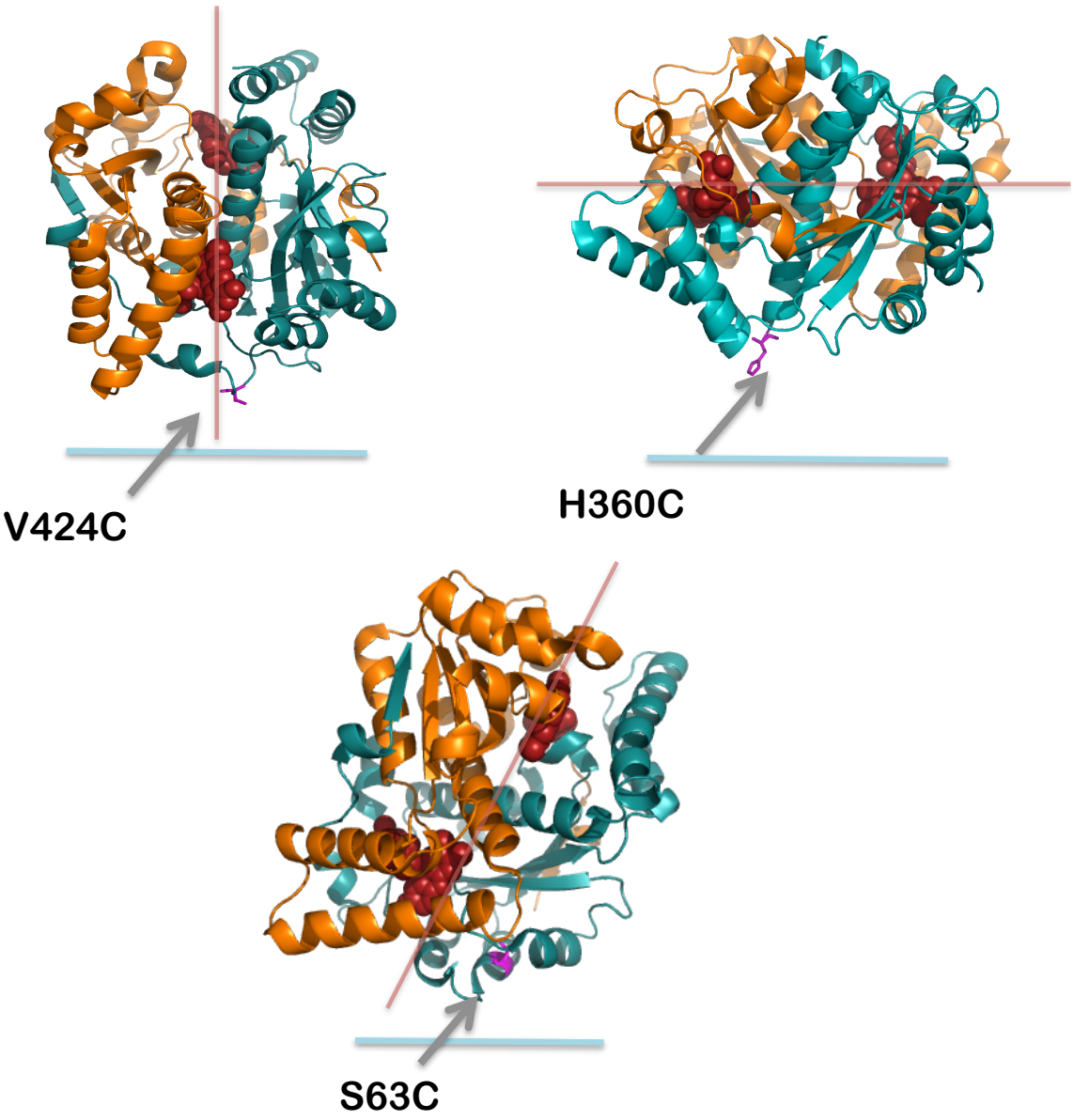

Figure 3.2. Structures of NfsB Variants
Structure of NfsB-V424C and NfsB-H360C with anchoring cysteine residues on loop regions. SAM surface represented in blue and active sites with red FMN cofacotrs. S63C-NfsB structure with anchoring cysteine residue on an α-helix

the previous chapter experiments were reported on NfsB-H360C and NfsB-V424C (Figure 3.2) constructs that have cysteine residues placed on loop structures. The assumption was that making a mutation on a loop is less likely to lead to problems with expression and folding of the enzyme. However, having the anchoring residue on a loop allows the immobilized enzyme to adopt a greater range of orientations with respect to the surface. In this chapter we describe the design of a construct with the cysteine residue on an α-helix to determine the effects of immobilizing the enzyme through a more rigid secondary structure element, thus reducing flexibility on the surface. S63C-NfsB was designed with the cysteine residue adjacent to one active site (Figure 3.2). T ½ and activity assays (Materials and Methods Chapter section 5.12 and 5.13) were performed on S63C-NfsB and compared to results from H360C and V424C NsfB constructs to learn more about the role of the tethering site on stability and activity.

3.2 Results

3.2.1 Mixed Surfaces

In these experiments we first investigated the effects of changing the mole ratios of EG_3-MAL:EG_3-OH or EG_3-MAL: EG_3-ME that comprise the SAM surface. We diluted EG_3-MAL linkers with EG_3-ME and EG_3-OH terminated linkers during the functionalization process creating 6 different SAM surfaces. Initially we determined the maleimide concentration range necessary for sufficient protein binding. If the maleimide concentration is too low, then protein binding will also be too low

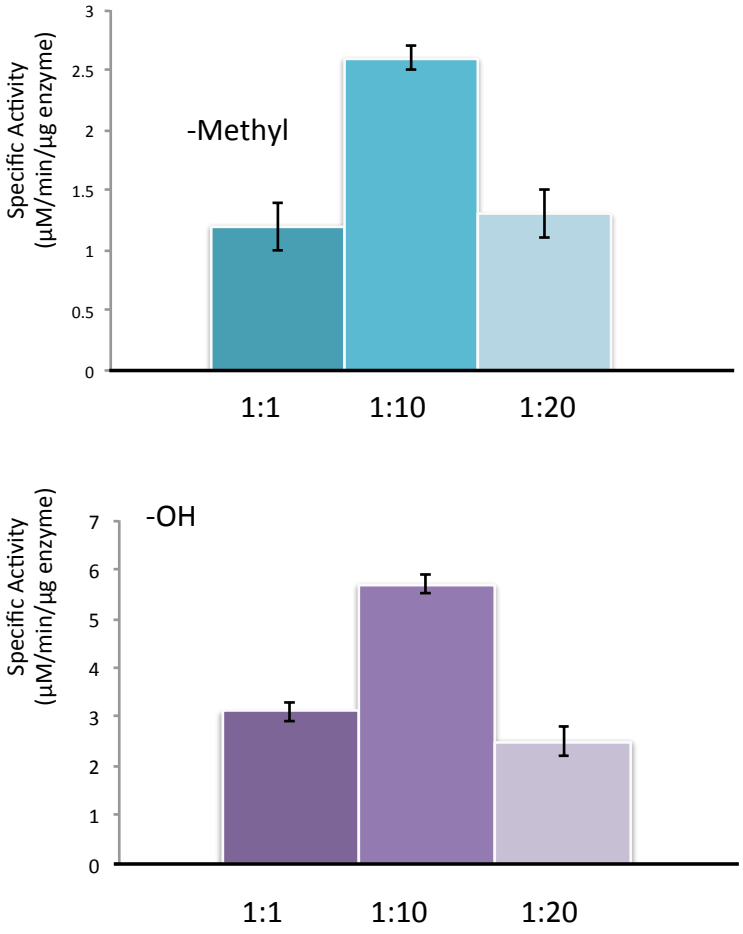

Figure 3.3. Specific Activity of Immobilized NfsB on –OH and –Methyl functionalized SAM surfaces

Specific activities at 1:1, 1:10 and 1:20 mole ratios of maleimide to –methyl (top) and maleimide to –OH (bottom)

resulting in the surface concentration and activity being too low to detect. We started by creating three different SAM surfaces with a 1:1, 1:10 and 1:20 mole ratio of EG_3-MAL to either EG_3-ME or EG_3-OH linkers. Based on an approximate diameter of 6 Å for EG_3-maleimide and 2 Å for EG_3-OH or EG_3-methyl terminated linkers, for a 1:1 ratio mixed surface this should result in ~1.2 maleimide groups per 10 $Å^2$. For a 1:10 ratio mixed surface ~0.12 maleimide groups should be attached per 10 $Å^2$. For a 1:20 ratio mixed surface ~0.061 maleimide groups per 10 $Å^2$.

We measured the specific activity for NfsB bound to each of the EG_3-OH and EG_3-ME functionalized SAM surfaces. The results for these assays are shown in Figure 3.3. The 1:10 mole ratio of EG_3-MAL:EG_3-OH or EG_3-MAL:EG_3-ME resulted in

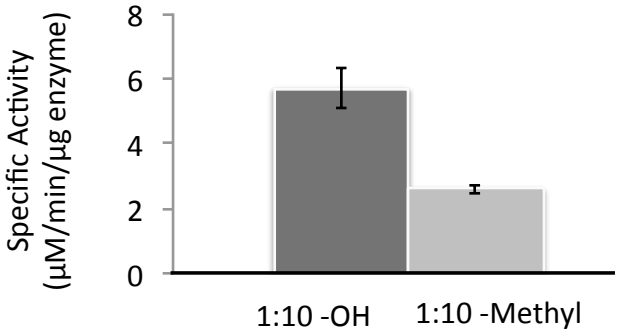

Figure 3.4. Specific Activity of Immobilized Enzyme Comparing –OH and -Methyl Functionalized SAM Surfaces
Comparison of specific activity of immobilized NfsB-V424C on 1:10 mole ratio of maleimide to –OH and –Methyl functionalized SAM surface

the highest specific activities and were measured as 5.7±0.6 μM/min/μg and 2.6±0.1 μM/min/μg respectively (Figure 3.4). The 1:10 ratio resulted in the highest specific activities. However, in all cases, the specific activities on the EG_3-MAL-EG_3-OH SAM surfaces were higher than the specific activities on the EG_3-MAL-EG_3-ME SAM surfaces. This shows that the EG_3-MAL-EG_3-OH SAM surface supports the retention of the structure and function of the immobilized NfsB.

3.2.2 Stability

One of the objectives of these experiments is to gain insight on the effects of mixed SAM surfaces and orientation on the stability of the enzyme. Our approach was to correlate thermal stability with immobilized enzyme activity. First we measured the T ½ of NfsB in solution. The fraction activity vs temperature plot is shown in Figure 3.5. The T ½ for NfsB in solution was found to be 45±2°C. Next we

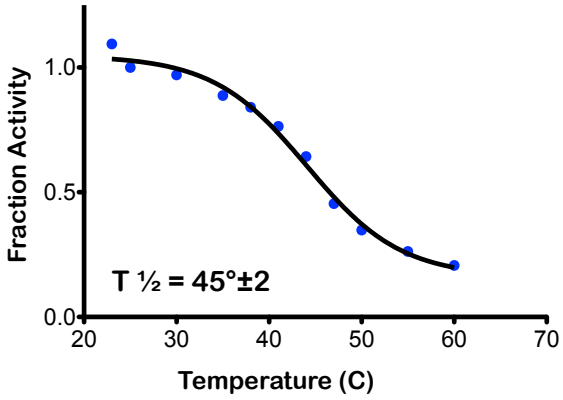

Figure 3.5. Thermal Melt Curve for NfsB in Solution
Fraction activity as a function of temperature (C) for NfsB-V424C in solution

measured the T ½ for immobilized NfsB. Both NfsB-V424C and NfsB-H360C orientations were bound to a 1:10 EG_3-MAL: EG_3-OH terminated SAM surface because this ratio gave the highest specific activity. The fraction activity vs

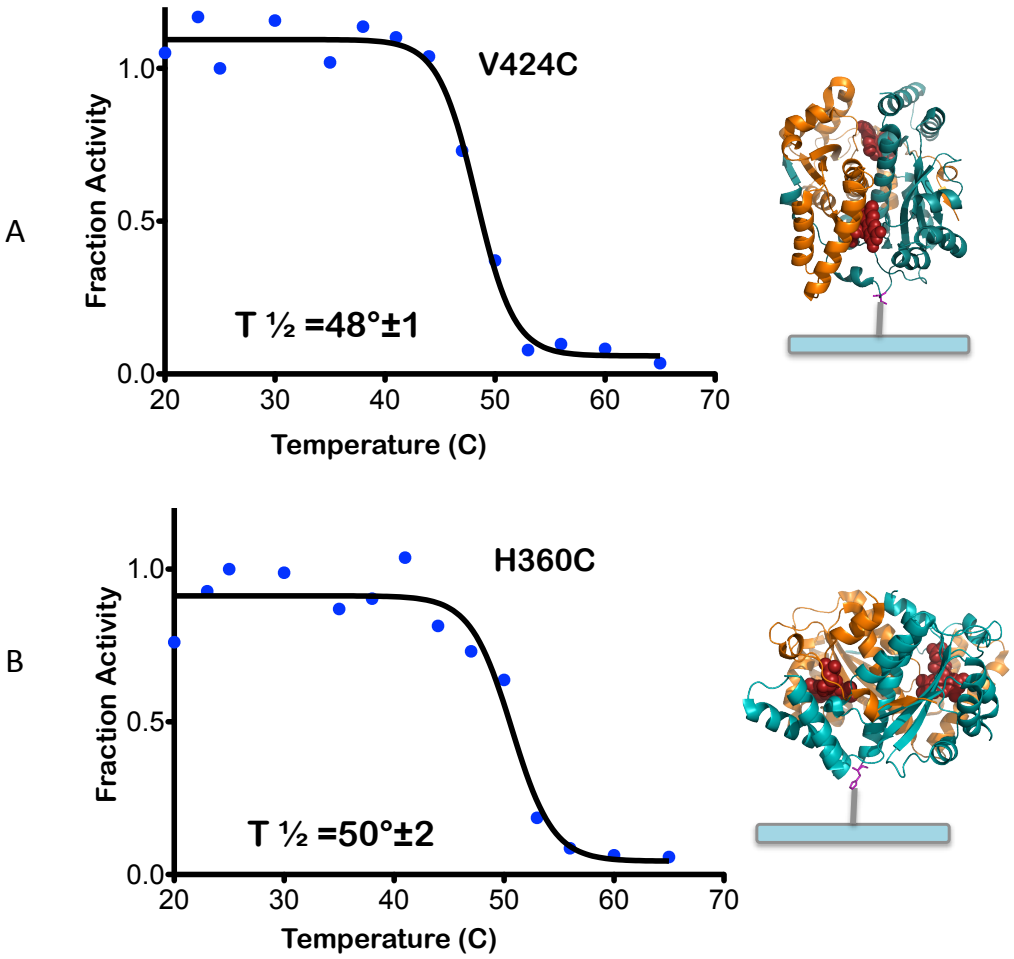

Figure 3.6. Thermal Melt Curve for Immobilized NfsB

A)Thermal melt curve for immobilized NfsB-V424C on 1:10 EG_3-MAL:EG_3-OH SAM surface. B) Thermal melt curve for immobilized NfsB-H360C on 1:10 EG_3-MAL:EG_3-OH SAM surface

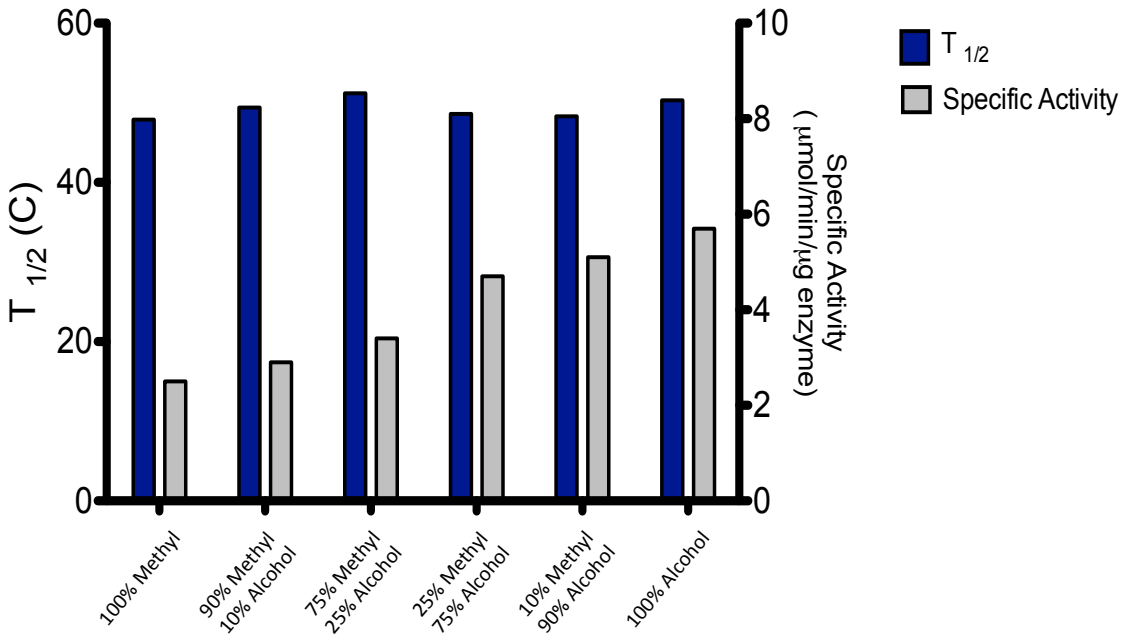

Figure 3.7. Specific Activities and T ½ Values for Immobilized NfsB on Varied SAM Surfaces
T ½ and specific activity values for NfsB-V424C immobilized on SAM surfaces functionalized with EG_3-MAL at a constant concentration and varying EG_3-OH and EG_3-ME concentrations

temperature plots are shown in Figure 3.6. NfsB-V424C T ½ was measured as 48±1°C and NfsB-H360C T ½ was measured as 50±2°C. These two values are the same within error. The thermal melt curves for NfsB in solution and immobilized NfsB show a change such that the curves are much sharper for immobilized NfsB which indicates a greater retention of activity for immobilized NfsB for temperatures between about 30 °C and 45 °C.

To expand on these experiments and learn more about the protein surface interactions we measured the T ½ and specific activity of NfsB-V424C immobilized on each of the six SAM surfaces with 1.2 nmol/g beads EG_3-MAL and varying percentages of EG_3-OH and EG_3-ME. The results are shown in Figure 3.7. The T ½ values remain within error over the range of mixed surfaces with an average value of 47 °C. The specific activity, however, does change over the range of mixed surfaces. The lowest specific activity is on the 100% EG_3-ME surface at 2.5 μM/min/μg enzyme. The specific activity increases with the increase of EG_3-OH on the SAM surface. This supports the previous results showing that the hydrophilic surface supports the retention of the structure and function of immobilized NfsB.

3.2.3 Loop vs Helix

NfsB-V424C and NfsB-H360C constructs position the cysteine residue on loop structures. For the following experiments we wanted to determine if placing the cysteine on a more rigid secondary structure element could produce additional stability for the immobilized enzyme. NfsB-S63C was designed for this purpose with

the cysteine residue residing at one end of an α-helix. This construct was expressed and purified in a similar manner to the loop constructs (Materials and Methods Chapter section 5.2 and 5.3). The specific activity in solution was found to be 25±2 μM/min/μg, which is comparable to the loop constructs with 24±1 μM/min/μg for NfsB-V424C and 27±1 μM/min/μg for NfsB-H360C.

NfsB-S63C was bound to a 1:10 mole ratio EG_3-MAL:EG_3-OH SAM surface. The specific activity was measured for immobilized NfsB-S63C and was found to be 5.6±0.3 μM/min/μg (Figure 3.8). The stability was measured for this variant on a 1:10 mole ratio EG_3-MAL:EG_3-OH SAM surface and the results are shown in Figure 3.8. The T ½ was measured at 50±1°C which is within error of the T ½ for NfsB-V424C and NfsB-H360C on the same SAM surface.

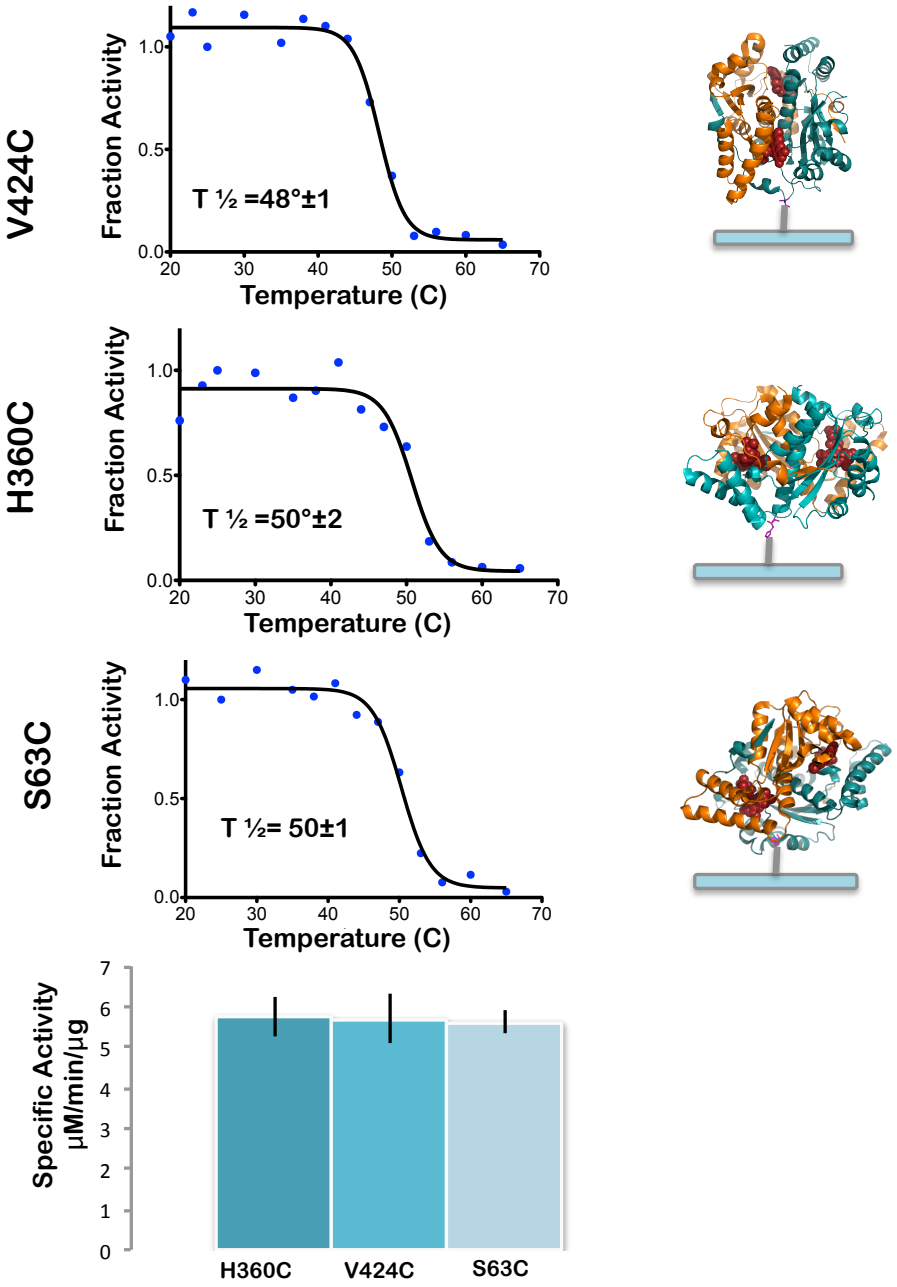

Figure 3.8. Thermal Melt Curve for Immobilized NfsB Variants

Thermal melt curve for immobilized NfsB-V424C, NfsB-H360C, NfsB-S63C, on 1:10 EG_3-MAL:EG_3-OH SAM surface with structure diagrams indicating orientation and specific activity graph

3.3 Discussion

The main objective of these experiments was to learn more about the effects that the attachment site and surface composition have on immobilized enzyme activity and stability. These studies utilized SAM surfaces functionalized with EG_3-MAL, EG_3-OH and EG_3-ME terminated linkers. We found that for mixed surfaces a mole ratio of 1:10 EG_3-MAL:EG_3-OH and EG_3-MAL:EG_3-ME resulted in a significantly higher specific activity compared to a 1:1 or 1:20 mole ratio. This result shows that there is an optimal surface composition for specific activity. The 1:10 mole ratio of EG_3-MAL:EG_3-OH or EG_3-MAL:EG_3-ME , could perhaps make the spacing between enzymes optimal, thereby decreasing unfavorable interaction between the enzymes and the surface. Based on this information, subsequent experiments were performed on 1:10 mole ratio mixed surfaces to ensure maximum activity. When comparing mixed surfaces, we found NfsB immobilized on an EG_3-OH functionalized SAM surfaces to have nearly double the specific activity compared to enzymes immobilized on a EG_3-ME functionalized SAM surfaces.

Stability has an important impact on the reuse, storage and optimal temperatures for an immobilized enzyme. In these experiments, T ½ was used as a measure of thermal stability. We found an increase in T ½ upon immobilization. However, when comparing orientation using NfsB-H360C and NfsB-V424C we did not find a change in T ½ . This shows that the change in orientation between the two constructs did not seem to affect stability and that when designing a construct for maximum stability the orientation doesn't appear to be a main concern.

To expand upon these experiments we made a range of mixed surfaces with both EG_3-ME and EG_3-OH with EG_3-MAL held at a constant concentration. These mixed surfaces were used to explore the relationship between surface hydrophobicity and the activity/stability of the immobilized enzyme. T ½ and specific activities were measured for immobilized NfsB across the range of mixed surfaces. T ½ remained constant, within error, across all the mixed surfaces. This suggests that this range of change in hydrophobicity, from a 73.4 ° contact angle for the EG_3-ME functionalized surface to a 53.3 ° contact angle for the EG_3-OH functionalized surface does not have an impact on the stability of immobilized enzyme. We do not interpret this result to mean that hydrophobicity of the surface does not affect stability, but rather that the range of hydrophobicity we tested did not affect stability. In future experiments, we plan on testing a wider range of hydrophobicity.

The hydrophobicity in this case did, however, affect specific activity. From 100% EG_3-ME surface to 100% EG_3-OH surface the specific activity nearly doubles. The specific activity increases with each increase of alcohol terminated PEG linker on the surface. This is evidence that surface composition does have an affect on specific activity of immobilized enzyme and opens the door for future experiments testing more types of surfaces. This is also consistent with our findings presented in Chapter 2, with the silane-EG_4-maleimide, that the surface itself plays an extremely important role for the activity of immobilized enzyme. It would be interesting to test if a more hydrophilic surface, perhaps functionalized with acid terminated PEG

linkers, will continue to get higher specific activities and at what point the trend stops.

In previous experiments, the NsfB constructs utilize cysteine tether sites located on loop structures. We hypothesized that immobilizing on a loop structure would give the enzyme a greater range of movement about the flexible loop and that immobilizing on a more rigid helix structure would give the immobilized enzyme less range of motion and more stability. The NfsB-S63C construct used in these experiments places the cysteine on an α-helix. We found that the specific activity of immobilized NfsB-S63C was the same as NfsB-H360C and NfsB-V424C on a 1:10 EG_3-MAL:EG_3-OH SAM surface. Similarly, the T ½ was also the same as the other constructs. This means, that at least in this case, placing the anchor point on a helix neither conferred any additional stability to the immobilized enzyme, nor reduced the specific activity. It is important to note here that other experiments done in our lab with a different enzyme β-galactosidase (β-gal) produced very different results in similar experiments. For example, when β-gal was immobilized through an α-helix the T ½ was the same as the T ½ in free solution while when immobilized through a loop region there was a greater than 10 °C reduction in the T ½[53]. This suggests that for β-gal immobilization through an α-helix had a destabilizing effect which is quite different from what we see with NfsB. Taken together we interpret this to mean that with enzyme immobilization there are often protein specific effects.

We found that the helix cysteine did cause this construct to bind more readily to the glass surface, giving higher surface concentration with a lower binding

concentration than the other constructs. This suggests that when designing a construct for maximum binding in mind, placing the anchor point on a more rigid secondary structure element can be helpful.

Chapter 4

Stability Through Surface Crowding and Co-immobilization

4.1 Introduction

One aspect of enzyme immobilization, which has been seldom reported in the literature for covalent immobilization, is the effect of surface crowding or surface density on the activity and stability of bound enzyme. Here, we define the surface density/crowding as the amount of immobilized enzyme in a particular portion of surface area. This is an important criterion because of the potential impact on the activity and stability of the immobilized enzyme. For example, we showed in Chapter 2 that there was a significant reduction in specific activity for enzyme immobilized on OTS, which had a much higher surface density than would be consistent with a monolayer. Caseli and co-workers[54] showed that in an adsorption system on Langmuir-Blodgett films, immobilized alkaline phosphatase had maximal activity at a surface density of 179 ng/cm^2 even though the highest surface density achieved was 1541 ng/cm^2. These negative effects on activity at higher surface densities could arise for a number of reasons such as impeded access of substrate to the active sites of tightly packed immobilized enzyme, impeded diffusion of product molecules, or partial unfolding or distortion of the enzymes structure based on electrostatic interactions. Another reason surface density is important for

immobilization is the ability to create a surface with high reproducibility and homogeneity[55]. This chapter explores the effects of surface crowding on our SAM surfaces by controlling the enzyme density on the surface.

As described in Chapter 2, short-chain ethylene glycols are the foundation of our SAM surfaces because they are hydrophilic and minimize non-specific protein adsorption, which is an ideal feature for covalent enzyme immobilization[56]. PEG is highly soluble in both aqueous and organic solvents and can be customized in both size and functionality[57]. A number of studies reported in the literature have used PEG-protein conjugates to change the properties of the protein. For example, PEG-insulin conjugates have been made that improve the stability of exogenous therapeutic insulin while maintaining its activity in a biological setting[58]. Trypsin-PEG conjugates have been created that prohibit precipitation when exposed to anti-trypsin antibody while maintaining catalytic activity[59]. In this chapter we investigated the effects of covalently binding higher molecular weight PEG to the SAM surface instead of the protein surface. We also measured the stability effects of co-immobilization with poly-sorbitol.

4.1.2 Changing Surface Density

For these experiments we first define what surface density a monolayer of protein would comprise. For our purposes, we use the diameter of NfsB (5 nm) as a basis for determining the parameters of a monolayer (diagram in Figure 4.1). We

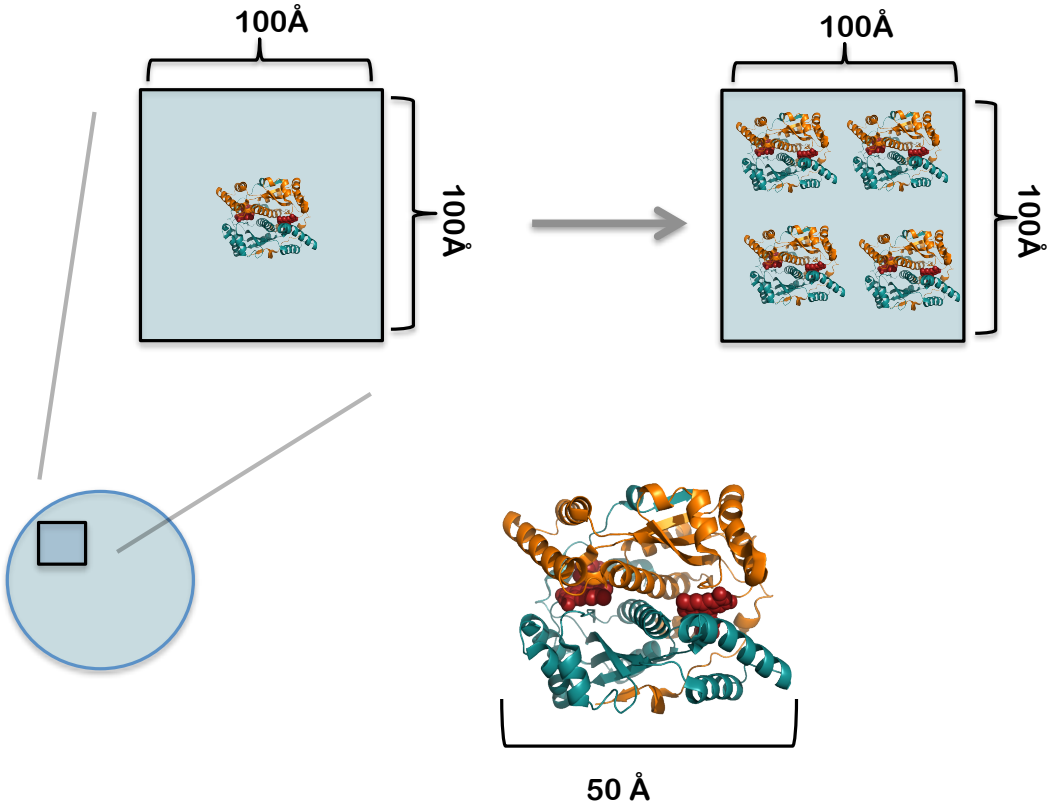

Figure 4.1. Monolayer Limits
Diagram of monolayer range limits and structure indicating the approximate diameter of NfsB. 1 enzyme in 10,000 $Å^2$ is equivalent to 26 ng enzyme/mg beads and 4 enzymes in 10,000 $Å^2$ is equivalent to 102 ng enzyme/mg beads.

define a diffuse monolayer as one enzyme in a 10,000 $Å^2$, which is equivalent to approximately 26 ng enzyme per mg glass beads. The upper limit, of what would be a densely packed monolayer, we define as 4 enzyme molecules in a 10,000 $Å^2$, which is equivalent to approximately 102 ng enzyme per mg glass beads.

For the experiments changing surface density, NfsB was immobilized on a 1:10 EG_3-MAL:EG_3-OH SAM surface prepared on 75 µm glass beads (Materials and Methods Chapter section 5.7). The glass beads were first silanized in toluene with silane-alkyne (0.1%). Unbound silane-alkyne was washed away with toluene followed by DMSO. EG_3-MAL (1.1 nmol/g beads) and EG_3-OH (10.9 nmol/g beads) were attached to the alkyne functionalized beads in a click reaction in 50% DMSO in DI water with 1 mM copper sulfate and 50 mg mL^{-1} sodium ascorbate gently agitating overnight at room temperature. The beads were then washed with DMSO 3 times followed by rinsing with DI water 3 times followed by incubation with 0.5 M EDTA for at least an hour to eliminate excess copper. Finally the beads were washed with PBS before enzyme immobilization.

NfsB-V424C, NfsB0-H360C and NfsB-S63C were immobilized to the prepared SAM surfaces (Materials and Methods Chapter section 5.10) by incubating overnight at 4 °C with gentle agitation. To achieve different surface densities, the concentration of enzyme was varied between 50 nM and 750 nM. With the range established above as a guide, the specific activity and T ½ was measured for NfsB-H360C, NfsB-V424C, and NfsB-S63C at different surface densities.

4.1.3 PEG Surface Modification

We modified the SAM surface with EG_{20} and EG_{40} to determine the effects on the activity and stability of immobilized NfsB. These modified surfaces were prepared using two different methodologies. First, thiol terminated EG_{20} and EG_{40} were immobilized with NfsB to a 1:10 EG_3-MAL:EG_3-OH SAM surface that was prepared as described above and also in the Materials and Methods Chapter. Thiol-EG_{20} and thiol-EG_{40} were then bound to the prepared SAM beads along with the enzyme at 4 °C, overnight with gentle agitation. For the 10% EG_{20} or EG_{40} surfaces the binding concentrations were 0.5 μM thiol-EG_{20} or thiol-EG_{40} and 4.5 μM NfsB. For the 1% surface the binding concentrations were 0.05 μM thiol-EG_{20} or thiol-EG_{40} and 4.95 μM NfsB.

The second methodology for PEG surface modification was to functionalize the silane-alkyne surface with EG_{20} in the click reaction as described above. The click reaction conditions were the same as described above, with the exception of the linker concentrations. For the 10% azido-EG_{20} surface the linker concentrations used were 1.2 nmol azido-EG_3-MAL, 1.08 nmol azido-EG_{20}, and 9.72 nmol azido-EG_3-OH per gram of beads being functionalized. For the 1% surface the click reaction contained 1.2 nmol azido-EG_3-maleimide, 0.108 nmol azido-EG_{20}, 10.7 nmol azido-EG_3-OH per gram of beads functionalized. All washing steps were performed as described above. Enzyme was then immobilized to these surfaces at 5 μM, in PBS at 4 °C overnight with gentle agitation. Unbound enzyme was washed away with 5% Tween-20 in PBS, followed by 3 PBS washes. The specific activities and T ½ values were measured for each sample.

4.1.4 Sorbitol Co-immobilization

Poly-sorbitol methacrylate (PMSA, thiol terminated, average MW 200 KD, obtained from Dr. Qiuming Wang) was co-immobilized with NfsB to investigate the polymer's effect on enzyme stability. These studies were done on 1:10 EG_3-MAL:EG_3-OH SAM surfaces. The preparation of these SAM surfaces was performed in the same manner as described above. The enzyme and PMSA were co-immobilized to the SAM surface, by mixing with the beads at 4°C overnight with 500 nM PMSA and 4.5 μM NfsB-V424C or NfsB-H360C. The specific activity and T ½ were measured for both NfsB variants.

4. 2 Results

4.2.1 Changing Surface Density

We originally proposed to control the surface density of immobilized enzyme in one of three ways. The simplest way was to prepare the SAM surfaces in exactly the same way, keep the enzyme concentration the same in the immobilization step and reduce the amount of enzyme bound to the surface by reducing the time it was allowed to bind. This approach did not work with NfsB because samples that were bound for shorter times did not contain sufficient protein for activity assays.

Another approach to change surface density was to change the amount of EG_3-maleimide bound to the surface when making the SAMs. This approach, however, would result in changing the overall composition of the SAM surface. In

order to avoid any complications that might arise from changing the surface composition, we chose another approach by changing the enzyme concentrations in the immobilization step as described in the introduction.

It is important to note that when changing the surface density of immobilized enzyme that each NfsB variant required slightly differing immobilization concentrations to achieve similar surface density. This aspect of immobilization is discussed further in the Materials and Methods Chapter section 5.10.

The range of surface coverage values fell between 15 ng/mg beads and 100 ng/mg beads. This range represents a diffuse monolayer (26 ng enzyme/mg beads) to a dense monolayer (102 ng enzyme/mg beads). Three NfsB variants were used for these experiments NfsB V424C, NfsB H360C, and NfsB S63C. The specific activity was measured for each NfsB variant at different surface coverages. Standard assay conditions were used, including 160 μM NADH, 500 μM 4-nitrobenzensulfonamide in PBS at room temperature. The change in absorbance at 340 nm was measured over 2 minutes to observe NADH consumption.

The results from these activity measurements are shown in Figure 4.2. NfsB-V424C had specific activity values that remained within error of each measurement over the range of surface coverage samples and had an average value of 5.6 μM/min/μg enzyme. NfsB-S63C behaved in a similar manner to NfsB-V424, with specific activity values that are all within error. The specific activity values for NfsB-S63C had an average value of 4.8 μM/min/μg enzyme. The specific activity values for NfsB H360C were not all within error. The lowest specific activity value was for

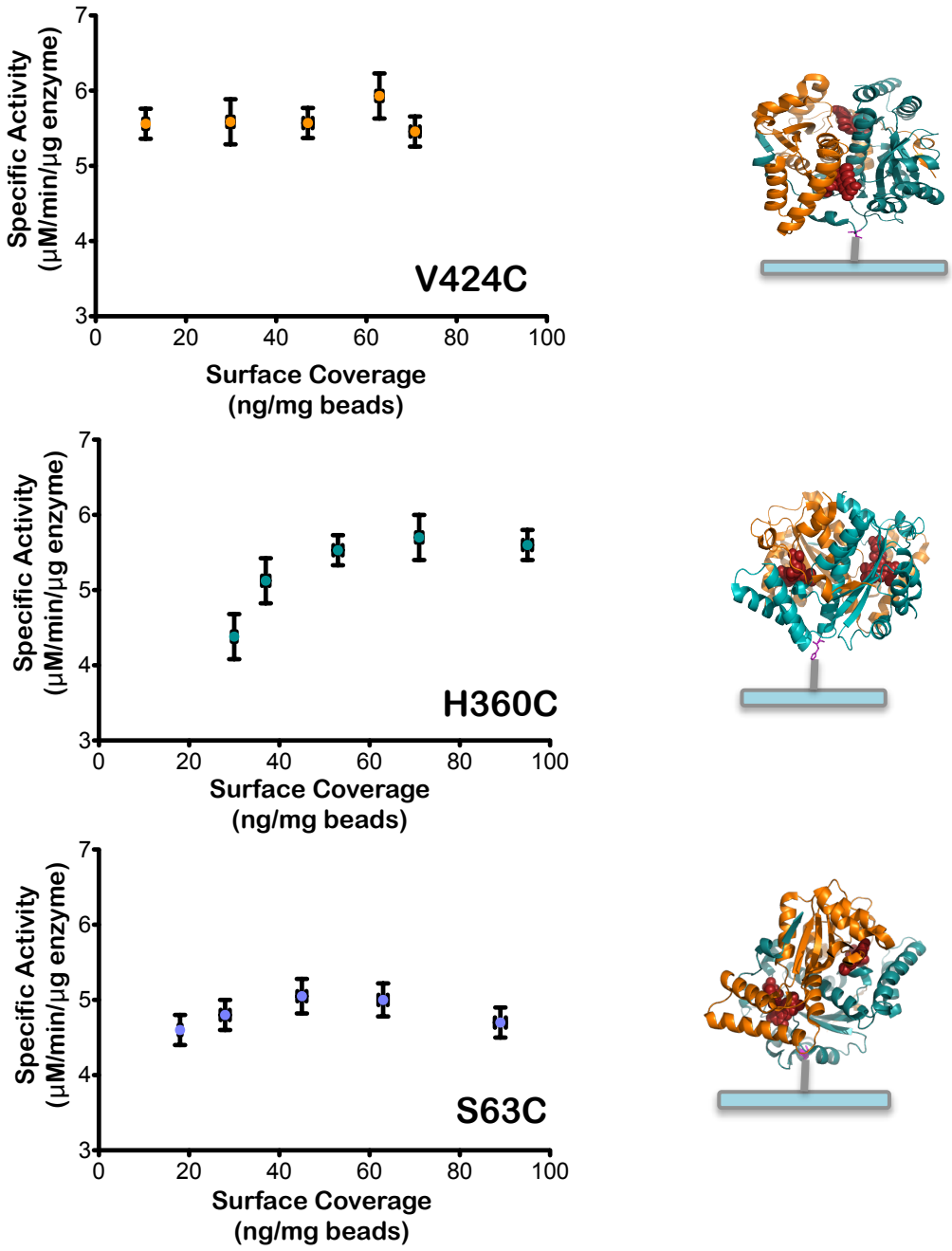

Figure 4.2. Specific Activity Measured on Different Surface Coverages
Specific activity as a function of surface coverage for V424C, H360C, and S63C NfsB variants. Surface attachment points are indicated in diagrams to the right.

the lowest surface coverage (30 ng/mg beads) at 4.4±0.3 μM/min/μg enzyme. The specific activity increases with the next increase of surface coverage and was measured at 4.7±.4 μM/min/μg enzyme for 37 ng/mg beads. The next three specific activity values then remain within error over the next three surface coverage values.

Thermal stability (T ½) was assessed for each NfsB variant over the range of surface coverage values. For the T ½ measurement, samples were heated to a particular temperature for 5 minutes and then brought to room temperature for 10 minutes before measuring the remaining activity (Materials and Methods Chapter section 5.13). The results from the T ½ measurements are shown in Figure 4.3. Over the range of surface coverage samples, NfsB-V424C had an average T ½ 49 °C. NfsB-S63C behaved in a similar fashion to NfsB-V424C, with the T ½ values being within error over the range of surface coverage values at an average temperature of 50 °C. NfsB-H360C unlike the V424C and S63C variants, had a sharp increase of T ½ values with the increase of surface coverage for the three lowest surface coverage values. For the three highest surface coverage samples, the T ½ values remained within error of each other. These specific activity and T ½ results are likely due to an orientation effect where the NfsB-H360C variant is susceptible to destabilization at lower surface density.

4.2.2 PEG Surface Modification

EG_{20} and EG_{40} SAM surfaces were created to study the effects of co-immobilization of higher molecular weight PEG linkers on immobilized NfsB. EG_{20} is approximately 6 nm long and EG_{40} is approximately 12 nm long. The length of these

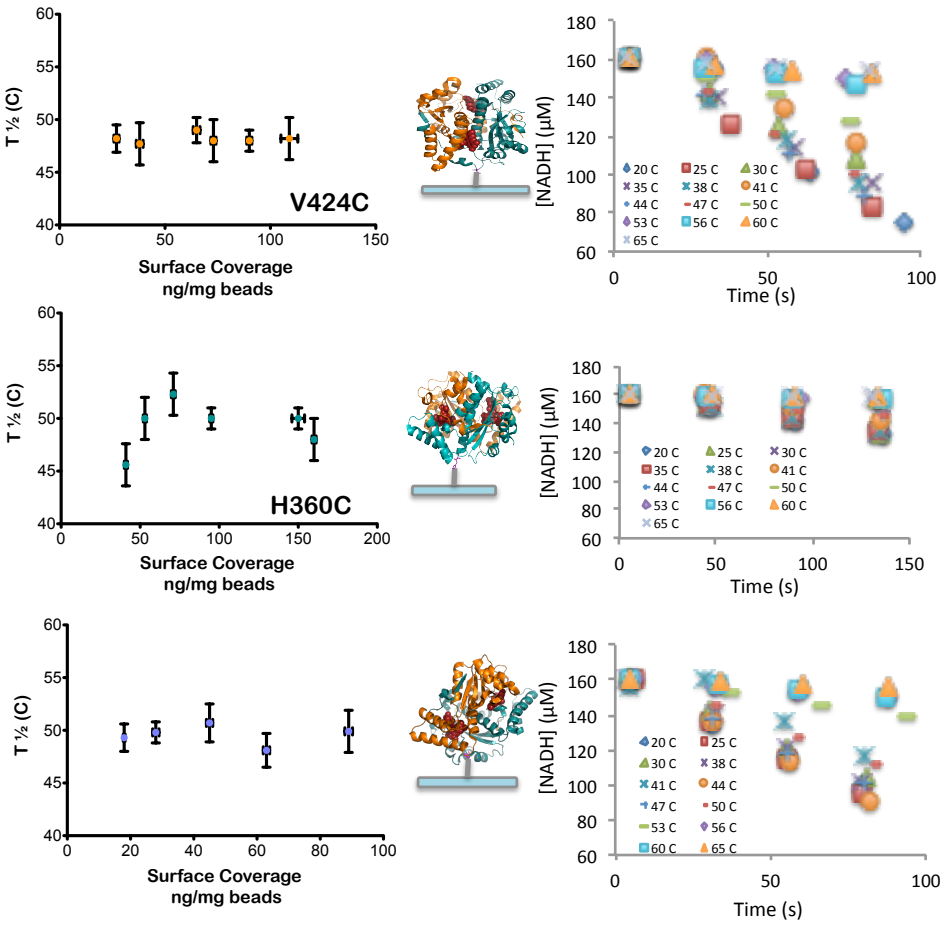

Figure 4.3. T ½ Values measured on Different Surface Coverages

T ½ values as a function of surface coverage for V424C, H360C, and S63C NfsB variants. Surface attachment points are indicated in diagrams in the center. NADH concentration as a function of time representative plots for V424C at 109 ng/mg beads, H360C at 41 ng/mg beads and S63C at 71 ng/mg beads.

PEG linkers allows them to extend above the maleimide layer and potentially interact with the immobilized enzyme. Experiments with thiol-EG_{20} and thiol-EG_{40} were performed on 1:10 mole ratio of EG_3-MAL:EG_3-OH SAM surfaces. The specific activity and T ½ were measured for each, and the results are shown in Table 4.1.

Table 4.1. Specific Activity and T ½ values for NfsB-H360C and NfsB-V424C variants co-immobilized with EG_{40} and EG_{20} linkers

SAM Surface	NfsB Variant	Specific Activity (μM/min/μg enzyme)	T 1/2 (°C)	Surface Coverage (ng enzyme/mg beads)
1% Thiol-PEG_{40}	H360C	3.2±0.4	48 ± 2	60
1% Thiol-PEG_{40}	V424C	3.9±0.3	50 ± 2	41
10% Thiol-PEG_{20}	H360C	2.1±0.2	47 ± 2	44
10% Thiol-PEG_{20}	V424C	2.5±0.3	48 ± 2	52

Experiments with azido-EG_{20} were performed by functionalizing the surface with the azido-EG_{20} at the click chemistry step of SAM surface preparation (Materials and Methods Chapter section 5.7). NfsB-V424C and NfsB-H360C was then bound to the prepared surfaces (5 μM, shaking 4 °C, overnight). The specific activities and T ½ values were measured for NfsB-V424C and NfsB-H360C on both 1% and 10% EG_{20} SAM surfaces. The results are shown in Table 4.2.

Another approach used to investigate the effects of longer PEG linkers was to use a silane-EG_{40}-maleimide linker. In this case, beads treated with piranha solution were then functionalized with silane-EG_{40}-maleimide (Nanocs, 2K PG2-ML-SL-2K) in toluene, shaking overnight. Beads were rinsed with toluene, followed by DMSO, followed by PBS buffer. Beads were then incubated overnight, 4°C with NfsB-V424C.

Table 4.2. Specific activity and T ½ values for NfsB-H360C and NfsB-V424C variants on Azido-EG_{20} SAM surfaces

SAM Surface	NfsB Variant	Specific Activity (μM/min/μg enzyme)	T 1/2 (°C)	Surface Coverage (ng enzyme/mg beads)
1% Azido-PEG_{20}	H360C	4.0±0.4	49 ± 1	71
1% Azido-PEG_{20}	V424C	2.7±0.3	49 ± 2	82
10% Azido-PEG_{20}	H360C	4.34±0.1	51 ± 2	92
10% Azido-PEG_{20}	V424C	2.54±0.1	49 ± 2	87

After washing away the excess, we measured the protein concentration and found that it was below the detectable limit or non-existent. We also measured catalytic activity and found it was also below the detectible limit or non-existent as would be expected based on the protein concentration measurement. Based on these measurements we determined that enzyme did not bind to this SAM surface.

4.2.3 Sorbitol Co-immobilization

Experiments with PSMA were performed on the same 1:10 EG_3-MAL:EG_3-OH SAM surfaces. The enzyme and PMSA were co-immobilized to the SAM surface, by shaking with the beads at 4°C overnight with 500 nM PMSA and 4.5 μM NfsB-V424C or NfsB-H360C. The specific activity and T ½ were measured for both NfsB variants, with the results shown in Figure 4.4. The T ½ for NfsB-V424C was 49±1°C and for NfsB H360C it was 49±2°C, these are within error of the T ½ values seen previously.

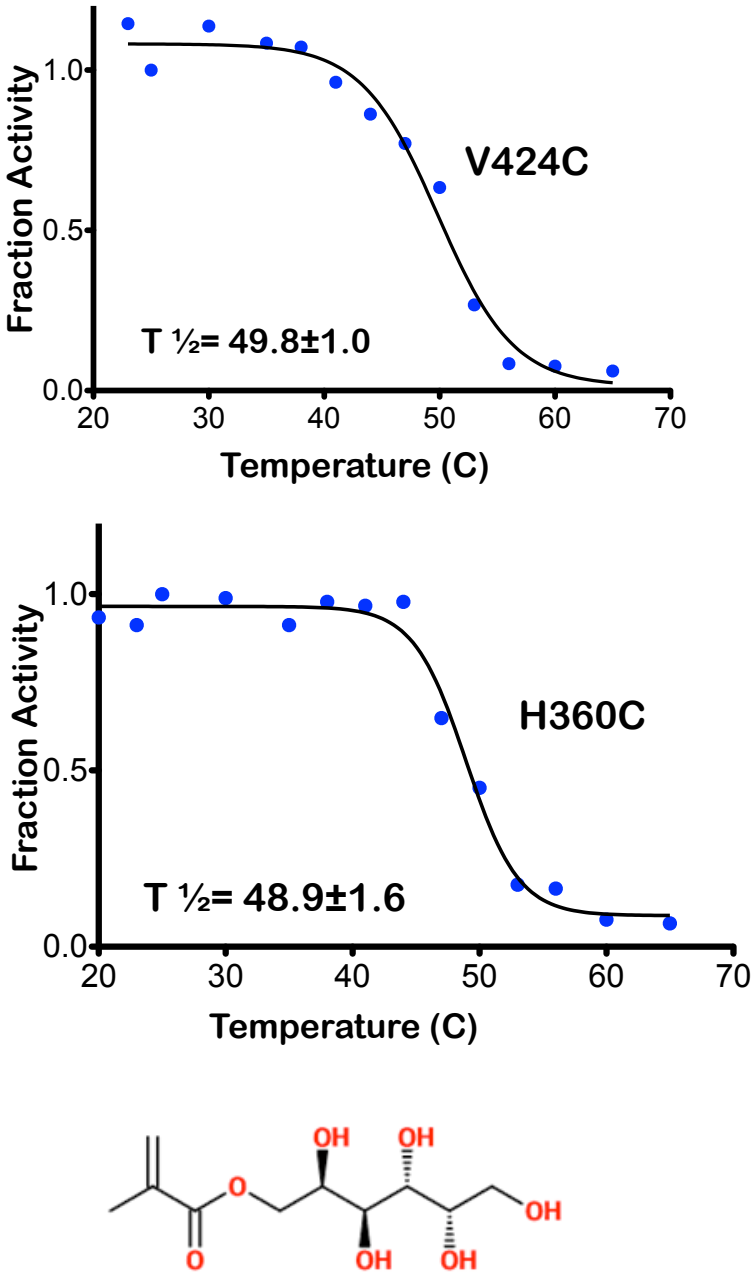

Figure 4.4. Thermal Curve for NfsB Co-Immobilized with PMSA
Fraction activity as a function of temperature for NfsB-V424C and NfsB-H360C NfsB variants co-immobilized with PMSA. Structure of sorbitol methacrylate monomer (bottom)

4.3 Discussion

The experiments described in this chapter were performed to enhance our understanding of the relationship between surface crowding or protein density and the effect it has on the catalytic activity and the stability of immobilized NfsB. We tested the specific activity of three NfsB variants under multiple surface coverage conditions from a sparse monolayer to a densely packed monolayer. Two NfsB variants V424C and S63C showed no change in specific activity arising from changes in the surface density. NfsB-H360C, however, showed about a 20% decrease in specific activity for lower surface density at 30 ng/mg bead coverage as compared to the specific activities at surface coverage densities higher than 53 ng/mg beads. When we looked at the stability via T ½ measurements we see a similar tendency where NfsB-V424C and NfsB-S63C don't show a change in T ½ over the range of surface density while NfsB-H360C again has a slight drop in T ½ values at the lower end of the surface density range with a T ½ of 46°C at a surface coverage of 41 ng/mg beads as compared to a T ½ of 52°C at a surface coverage of 71 ng/mg beads. The changes here are small, but indicate a potentially orientation dependent effect. One possible reason for this result is that at lower surface density NfsB-H360C could be interacting with the surface strongly enough to reduce activity and stability whereas at higher surface density these interactions with the surface are physically blocked from occurring by neighboring immobilized proteins. These results highlight an area where future experiments could be performed to determine if this

is an orientation effect. One way to do this would be to design another NfsB construct with different cysteine site that provides a similar orientation to see if these results would be replicated.

We made SAM surfaces with silane-EG_{40}-maleimide, however, the enzyme did not efficiently bind to this surface. We posit that this lack of binding is due to the fact that PEG is highly flexible in solution[3] so the longer PEG linker allows the maleimide-terminated end to fold over back towards the glass surface, sterically blocking enzyme binding. This indicates that choosing the appropriate size of PEG linkers is critical when employing this type of enzyme immobilization. More experiments could be done in this area to determine the limits of PEG linker size and possible benefits of using different sized linkers.

In this chapter we also examined co-immobilization of NfsB with EG_{20} or EG_{40} PEG linkers. We found that for both PEG lengths we see a reduction in specific activity. The reduction seems to be greatest for thiol-EG_{40} co-immobilized at 10%, which brings the specific activity to half of what we have seen on other SAM surfaces. For the azido-EG_{20} SAM surfaces, it appears the reduction in specific activity is greater for the NfsB V424C variant. This could indicate that the co-immobilization with the longer PEG molecules could be blocking the active site facing the surface. Surprisingly, on all of the EG_{20} and EG_{40} surfaces we do not see an effect on the T ½, which remains consistent in these experiments. Furthermore, the T ½ is also unaffected by the co-immobilization of PMSA.

The thermal melt curves we used in these experiments are only one of many

ways of assessing stability. It would be interesting to test these longer PEG surfaces in other denaturing environments such as organic solvents. Another aspect is that the PEG molecules used in these experiments are linear PEG-chains. PEG is available in many molecular weight and also ranges in branched versions. Assessing enzyme co-immobilized with higher molecular weight, especially branched PEG linkers, would be a logical next step for these experiments.

Chapter 5

Materials and Methods

5.1 NfsB Constructs

NfsB is natively expressed as a homo-dimer; a fusion protein was designed to connect the two monomers with a ten glycine residue linker. A native cysteine residue at position 85 was mutated to an alanine and the surface cysteine was placed at position 424. The *NfsB* fusion gene was commercially synthesized by GenScript (New Jersey) and was cloned in the pET28b bacterial expression vector with N-terminal his-tag and kanamycin resistance gene. The fusion gene was codon optimized to allow site directed mutagenesis to be used for subsequent construct design. Another NfsB version (DNA and protein) without the 10-glycine linker was also obtained for control purposes.

The Phusion Site-Directed Mutagenesis Kit from ThermoFisher Scientific was used to make three NfsB constructs. Parameters for primer design provided with the mutagenesis kit were followed. The cysteine at position 424 was mutated back to a valine, in order to create a cysteine free control. The histidine at position 360 was mutated to a cysteine for the H360C NfsB construct. The serine at position 63

NfsB-V424C

ATGGACATCATCTCGGTTGCACTGAAACGCCACTCTACGAAAGCATTTGACGCCTCGAAAAAACTGACCCCGGAA
CAAGCAGAACAGATTAAAACCCTGCTGCAGTATTCACCGAGCTCTACGAACTCGCAACCGTGGCATTTTATCGTG
GCGTCCACCGAAGAAGGCAAAGCGCGTGTCGCCAAATCAGCGGCCGGTAACTACGTGTTTAATGAACGCAAAATG
CTGGATGCAAGCCACGTGGTTGTCTTCGCAGCTAAAACGGCTATGGATGACGTTTGGCTGAAACTGGTGGTTGAT
CAGGAAGATGCAGACGGCCGTTTTGCAACCCCGGAAGCTAAAGCGGCCAATGACAAAGGTCGTAAATTTTTCGCC
GATATGCATCGCAAAGACCTGCACGATGACGCGGAATGGATGGCCAAACAAGTTTATCTGAACGTCGGCAATTTC
CTGCTGGGTGTTGCAGCTCTGGGCCTGGATGCAGTCCCGATTGAAGGCTTTGATGCGGCCATCCTGGACGCTGAA
TTCGGTCTGAAAGAAAAAGGCTACACGTCGCTGGTCGTGGTTCCGGTCGGTCATCACAGCGTGGAAGATTTTAAC
GCGACCCTGCCGAAATCTCGTCTGCCGCAGAATATTACCCTGACGGAAGTGGGTCAAGGTGGCGGCGGTGGTGGT
GGTGGTATGGATATTATCAGTGTTGCGCTGAAACGCCATTCCACGAAAGCATTTGACGCTAGCAAAAAACTGACG
CCGGAACAGGCCGAACAAATTAAAACGCTGCTGCAGTATAGCCCGAGTTCCACCAACTCTCAACCGTGGCATTTC
ATCGTGGCGTCGACGGAAGAAGGTAAAGCGCGTGTTGCCAAAAGCGCAGCTGGTAACTACGTCTTCAACGAACGT
AAAATGCTGGACGCGAGCCACGTCGTGGTTTTCGCGGCCAAAACGGCCATGGACGATGTTTGGCTGAAACTGGTC
GTGGATCAGGAAGATGCGGACGGCCGCTTCGCCACCCCGGAAGCTAAAGCAGCTAATGATAAAGGCCGCAAATTT
TTCGCGGACATGCACCGTAAAGATCTGCATGACGATGCCGAATGGATGGCGAAACAGGTGTATCTGAACGTTGGT
AATTTCCTGCTGGGTGTGGCAGCACTGGGTCTGGATGCCGTTCCGATTGAAGGTTTTGATGCAGCTATCCTGGAC
GCAGAATTCGGCCTGAAAGAAAAAGGTTACACCTCTCTGGTTGTCGTGCCGGTGGGCCATCACAGTTGCGAAGAT
TTCAATGCCACGCTGCCGAAATCACGCCTGCCGCAAAACATCACGCTGACCGAAGTCTAA

NfsB-C85A

ATGGACATCATCTCGGTTGCACTGAAACGCCACTCTACGAAAGCATTTGACGCCTCGAAAAAACTGACCCCGGAA
CAAGCAGAACAGATTAAAACCCTGCTGCAGTATTCACCGAGCTCTACGAACTCGCAACCGTGGCATTTTATCGTG
GCGTCCACCGAAGAAGGCAAAGCGCGTGTCGCCAAATCAGCGGCCGGTAACTACGTGTTTAATGAACGCAAAATG
CTGGATGCAAGCCACGTGGTTGTCTTCGCAGCTAAAACGGCTATGGATGACGTTTGGCTGAAACTGGTGGTTGAT
CAGGAAGATGCAGACGGCCGTTTTGCAACCCCGGAAGCTAAAGCGGCCAATGACAAAGGTCGTAAATTTTTCGCC
GATATGCATCGCAAAGACCTGCACGATGACGCGGAATGGATGGCCAAACAAGTTTATCTGAACGTCGGCAATTTC
CTGCTGGGTGTTGCAGCTCTGGGCCTGGATGCAGTCCCGATTGAAGGCTTTGATGCGGCCATCCTGGACGCTGAA
TTCGGTCTGAAAGAAAAAGGCTACACGTCGCTGGTCGTGGTTCCGGTCGGTCATCACAGCGTGGAAGATTTTAAC
GCGACCCTGCCGAAATCTCGTCTGCCGCAGAATATTACCCTGACGGAAGTGGGTCAAGGTGGCGGCGGTGGTGGT
GGTGGTATGGATATTATCAGTGTTGCGCTGAAACGCCATTCCACGAAAGCATTTGACGCTAGCAAAAAACTGACG
CCGGAACAGGCCGAACAAATTAAAACGCTGCTGCAGTATAGCCCGAGTTCCACCAACTCTCAACCGTGGCATTTC
ATCGTGGCGTCGACGGAAGAAGGTAAAGCGCGTGTTGCCAAAAGCGCAGCTGGTAACTACGTCTTCAACGAACGT
AAAATGCTGGACGCGAGCCACGTCGTGGTTTTCGCGGCCAAAACGGCCATGGACGATGTTTGGCTGAAACTGGTC
GTGGATCAGGAAGATGCGGACGGCCGCTTCGCCACCCCGGAAGCTAAAGCAGCTAATGATAAAGGCCGCAAATTT
TTCGCGGACATGCACCGTAAAGATCTGCATGACGATGCCGAATGGATGGCGAAACAGGTGTATCTGAACGTTGGT
AATTTCCTGCTGGGTGTGGCAGCACTGGGTCTGGATGCCGTTCCGATTGAAGGTTTTGATGCAGCTATCCTGGAC
GCAGAATTCGGCCTGAAAGAAAAAGGTTACACCTCTCTGGTTGTCGTGCCGGTGGGCCATCACAGTGTCGAAGAT
TTCAATGCCACGCTGCCGAAATCACGCCTGCCGCAAAACATCACGCTGACCGAAGTCTAA

Figure 5.1. NfsB V424C and C85A DNA Sequences

NfsB S63C

ATGGACATCATCTCGGTTGCACTGAAACGCCACTCTACGAAAGCATTTGACGCCTCGAAAAAACTGACCCCGGAA
CAAGCAGAACAGATTAAAACCCTGCTGCAGTATTCACCGAGCTCTACGAACTCGCAACCGTGGCATTTTATCGTG
GCGTCCACCGAAGAAGGCAAAGCGCGTGTCGCCAAATCAGCGGCCGGTAACTACGTGTTTAATGAACGCAAAATG
CTGGATGCAAGCCACGTGGTTGTCTTCGCAGCTAAAACGGCTATGGATGACGTTTGGCTGAAACTGGTGGTTGAT
CAGGAAGATGCAGACGGCCGTTTTGCAACCCCGGAAGCTAAAGCGGCCAATGACAAAGGTCGTAAATTTTTCGCC
GATATGCATCGCAAAGACCTGCACGATGACGCGGAATGGATGGCCAAACAAGTTTATCTGAACGTCGGCAATTTC
CTGCTGGGTGTTGCAGCTCTGGGCCTGGATGCAGTCCCGATTGAAGGCTTTGATGCGGCCATCCTGGACGCTGAA
TTCGGTCTGAAAGAAAAAGGCTACACGTCGCTGGTCGTGGTTCCGGTCGGTCATCACAGCGTGGAAGATTTTAAC
GCGACCCTGCCGAAATCTCGTCTGCCGCAGAATATTACCCTGACGGAAGTGGGTCAAGGTGGCGGCGGTGGTGGT
GGTGGTATGGATATTATCAGTGTTGCGCTGAAACGCCATTCCACGAAAGCATTTGACGCTAGCAAAAAACTGACG
CCGGAACAGGCCGAACAAATTAAAACGCTGCTGCAGTATAGCCCGAGTTCCACCAACTCTCAACCGTGGCATTTC
ATCGTGGCGTCGACGGAAGAAGGTAAAGCGCGTGTTGCCAAAAGCGCAGCTGGTAACTACGTCTTCAACGAACGT
AAAATGCTGGACGCGAGCCACGTCGTGGTTTTCGCGGCCAAAACGGCCATGGACGATGTTTGGCTGAAACTGGTC
GTGGATCAGGAAGATGCGGACGGCCGCTTCGCCACCCCGGAAGCTAAAGCATGTAATGATAAAGGCCGCAAATTT
TTCGCGGACATGCACCGTAAAGATCTGCATGACGATGCCGAATGGATGGCGAAACAGGTGTATCTGAACGTTGGT
AATTTCCTGCTGGGTGTGGCAGCACTGGGTCTGGATGCCGTTCCGATTGAAGGTTTTGATGCAGCTATCCTGGAC
GCAGAATTCGGCCTGAAAGAAAAAGGTTACACCTCTCTGGTTGTCGTGCCGGTGGGCCATCACAGTTGCGAAGAT
TTCAATGCCACGCTGCCGAAATCACGCCTGCCGCAAAACATCACGCTGACCGAAGTCTAA

NfsB H360C

ATGGACATCATCTCGGTTGCACTGAAACGCCACTCTACGAAAGCATTTGACGCCTCGAAAAAACTGACCCCGGAA
CAAGCAGAACAGATTAAAACCCTGCTGCAGTATTCACCGAGCTCTACGAACTCGCAACCGTGGCATTTTATCGTG
GCGTCCACCGAAGAAGGCAAAGCGCGTGTCGCCAAATCAGCGGCCGGTAACTACGTGTTTAATGAACGCAAAATG
CTGGATGCAAGCCACGTGGTTGTCTTCGCAGCTAAAACGGCTATGGATGACGTTTGGCTGAAACTGGTGGTTGAT
CAGGAAGATGCAGACGGCCGTTTTGCAACCCCGGAAGCTAAAGCGGCCAATGACAAAGGTCGTAAATTTTTCGCC
GATATGCATCGCAAAGACCTGCACGATGACGCGGAATGGATGGCCAAACAAGTTTATCTGAACGTCGGCAATTTC
CTGCTGGGTGTTGCAGCTCTGGGCCTGGATGCAGTCCCGATTGAAGGCTTTGATGCGGCCATCCTGGACGCTGAA
TTCGGTCTGAAAGAAAAAGGCTACACGTCGCTGGTCGTGGTTCCGGTCGGTCATCACAGCGTGGAAGATTTTAAC
GCGACCCTGCCGAAATCTCGTCTGCCGCAGAATATTACCCTGACGGAAGTGGGTCAAGGTGGCGGCGGTGGTGGT
GGTGGTATGGATATTATCAGTGTTGCGCTGAAACGCCATTCCACGAAAGCATTTGACGCTAGCAAAAAACTGACG
CCGGAACAGGCCGAACAAATTAAAACGCTGCTGCAGTATAGCCCGAGTTCCACCAACTCTCAACCGTGGCATTTC
ATCGTGGCGTCGACGGAAGAAGGTAAAGCGCGTGTTGCCAAAAGCGCAGCTGGTAACTACGTCTTCAACGAACGT
AAAATGCTGGACGCGAGCCACGTCGTGGTTTTCGCGGCCAAAACGGCCATGGACGATGTTTGGCTGAAACTGGTC
GTGGATCAGGAAGATGCGGACGGCCGCTTCGCCACCCCGGAAGCTAAAGCAGCTAATGATAAAGGCCGCAAATTT
TTCGCGGACATGCACCGTAAAGATCTGTGTGACGATGCCGAATGGATGGCGAAACAGGTGTATCTGAACGTTGGT
AATTTCCTGCTGGGTGTGGCAGCACTGGGTCTGGATGCCGTTCCGATTGAAGGTTTTGATGCAGCTATCCTGGAC
GCAGAATTCGGCCTGAAAGAAAAAGGTTACACCTCTCTGGTTGTCGTGCCGGTGGGCCATCACAGTTGCGAAGAT
TTCAATGCCACGCTGCCGAAATCACGCCTGCCGCAAAACATCACGCTGACCGAAGTCTAA

Figure 5.2. NfsB S63C and H360C DNA Sequences

was mutated to a cysteine for the S63C NfsB construct. All constructs were selected by kanamycin resistance and then confirmed by sequencing. The sequences of all the NfsB variants are shown in Figures 5.1 and 5.2

5.2 Expression

E. coli BL21(DE3) cells were transformed by electroportation with expression vectors containing NfsB genes. Starter-cultures were grown in LB media with kanamycin (50 μg mL^{-1}) overnight at 37 °C. Overnight cultures were then used to inoculate larger cultures grown in the presence of kanamycin (50 μg mL^{-1}) in 2XYT media at 37 °C with shaking at 200 rpm until reaching an OD of 0.6 at 600 nm. Once the cultures reached OD_{600} 0.6 the temperature was reduced to 18 °C and the cells were induced by the addition of isopropyl-β-D-1-thiogalactopyranoside (IPTG) (1mM final concentration) and allowed to grow overnight with continuous shaking. Cells were harvested by centrifugation (4 °C, 4000 g, 20 min) and stored at -20 °C.

5.3 Purification

Thawed cells were re-suspended in lysis buffer (100mM Tris, 300 mM NaCl, 1mM β-mercaptoethanol, 10% glycerol, complete EDTA-free protease inhibitor cocktail tablet (Roche), pH 8.0). Five mL of lysis buffer was used per gram of thawed cells. The cells were then lysed by sonication using a 2 second "on" 8 second "off" pulse sequence, at a total of 5 minutes "on" pulse time. The sonication step was always done on ice to reduce heating of the lysate. Cell debris was removed by centrifugation (4 °C, 14000 g for 60 minutes). The supernatant was incubated with 5

mL Ni-NTA resin (Thermo) at 4 °C with gentle agitation overnight. The Ni-NTA resin was then poured into a chromatography column and washed with 100 mL of 20mM imidazole in lysis buffer. The flow through was collected for all steps.

NfsB was eluted off the Ni-NTA resin using a step gradient of 50mM, 100mM, 150mM, 200mM and 250mM imidazole in lysis buffer (20mL each). Fractions were collected and then assessed for purity by running samples on an SDS-PAGE gel. The purest fractions were combined and dialyzed against 100mM Tris buffer with 300mM NaCl, 1mM tris(2-carboxyethyl)phosphine (TCEP), 10% glycerol, pH 7.5, overnight. The enzyme solution was then aliquoted into 0.5 mL aliquots in 1.5 mL polypropylene tubes, flash frozen in liquid nitrogen and stored at -80 °C. A purification performed from three liters of culture would typically yield around 50mL protein solution at a concentration of 100μM.

5.4 Protein Quantification

Protein concentrations were measured in solution by UV-Vis absorbance at 280nm. Concentrations were calculated using ε= 44920 $M^{-1}cm^{-1}$. This extinction coefficient was calculated based on the amino acid sequence using the proteomics server ExPASy[60].

5.5 Cysteine Quantification

Reactive surface cysteine residues were quantified using Ellman's reagent (5,5'-dithio-*bis*-(2-nitrobenzoid acid) or DTNB)). Ellman's reaction buffer was made of 0.1M sodium phosphate and 1mM EDTA at pH 8.0. Ellman's reagent was made by

dissolving 4mg DTNB in 1mL Ellman's reaction buffer. Samples were prepared by adding 50µL Ellman's reagent and 2.5mL Ellman's reaction buffer to a tube. 250µL protein sample was then added, mixed, and incubated at room temperature for 15 minutes. Absorbance for the samples was then measured at 412nm and quantified using a standard curve of cysteine.

It is important to note one thing about the Ellman's reagent quantification for NfsB. The absorbance spectrum for NfsB contains a peak for the bound FMN at around 450nm. The absorbance of the Ellman's reagent is at 412nm, so there was some amount of peak overlap. In order to avoid any interference of the FMN peak, FMN was removed from the NfsB samples prior to quantification. In order to do this, the protein was treated with 10% SDS and buffer exchanged using a centrifugal filter (Amicon, 10,000MW). SDS was removed by repeating the buffer exchange with a centrifugal filter (Amicon, 10,000MW) as well, before the Ellman's assay.

5.6 FMN Quantification

The FMN content, of purified NfsB samples, was quantified spectroscopically by absorbance at 444 nm. NfsB samples were denatured, removing FMN, then passed through 10,000 MW Amicon Centrifugal Filters. The flow through was used to measure FMN by UV absorbance using an extinction coefficient of 12,500 $M^{-1}cm^{-1}$.

5.7 Surface Functionalization

75-µm glass beads (Supelco, acid-washed) were prepared for functionalization by first being incubated with piranha solution. Piranha solution is

made by mixing 45mL concentrated sulfuric acid with 15mL hydrogen peroxide (13%). Beads were stirred periodically and allowed to incubate with piranha solution over night. The beads were then rinsed with copious amounts of DI water, until neutral pH as measured by pH paper (EMD Millipore). To remove all water from the beads, they were rinsed with dimethyl sulfoxide (DMSO) 4 times followed by 3 rinses with toluene. The Beads were silanized (shaking, overnight) in anhydrous toluene with silane-alkyne (Gelest, o-(propargyl)-N-(triethoxysilylpropyl) carbamate) at 0.1% where the liquid volume is 4 times the volume of beads being functionalized. The structure of the silane-alkyne linker is shown in Figure 5.3. Excess silane-alkyne reagent was removed by rinsing with toluene (3 times), followed by rinsing with DMSO (3 times).

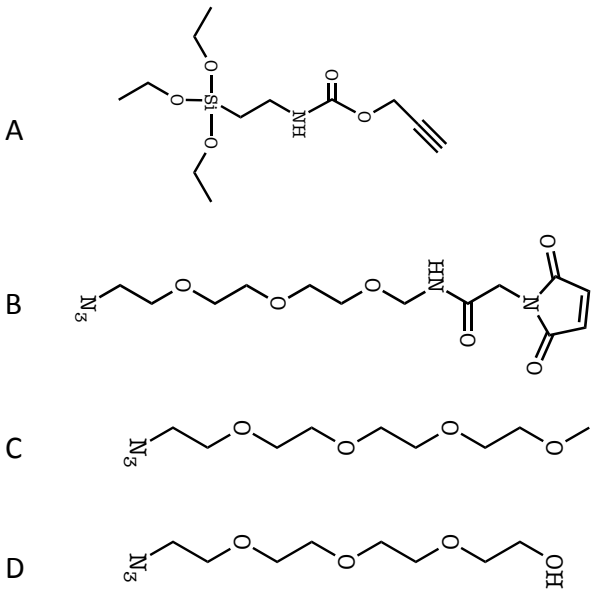

Figure 5.3.Structures of Linkers Used to Prepare SAM Surfaces
A) Silane alkyne linker, B) Azido-EG_3-maleimide linker, C) Azido-EG_3-methyl linker, D) Azido-EG_3-OH linker

PEG linkers were then attached to the alkyne-functionalized glass bead surfaces by a click reaction. The conditions used were as follows: 1 mM copper sulfate, 50 mg mL^{-1} sodium ascorbate in 50% DMSO in DI water. Click reactions were incubated overnight with shaking at room temperature after the addition of appropriate azido linkers. Azido-EG_3-Maleimide kit 25mg (Click Chemistry Tools, Arizona) was prepared by dissolving Azido-EG_3-amine in 1mL dry DMSO, then adding maleimide-NHS ester, and shaking at room temperature for 1 hour. 75 μm glass beads were functionalized with 12 nmol total linker per gram of beads. Using 12 nmol/g beads as the total amount of EG_3 linker, the values were adjusted appropriately to make listed mole ratios. For example, a 1:20 mole ratio EG_3-MAL:EG_3-OH would have 0.57 nmol/g beads EG_3-MAL and 11.4 nmol/g beads EG_3-OH. For mixed SAM surfaces with maleimide held at a constant at concentration 1.1 nmol/g beads (1:10) with the remaining 10.9 nmol changing appropriately for the percentage linkers listed. For example a EG_3-MAL surface with a 25% EG_3-ME-75% EG_3-OH surface would have: 1.1 nmol/g beads EG_3-MAL, 2.73 nmol/g beads EG_3-ME, and 8.17 nmol/g beads EG_3-OH. Structures for azido-linkers are shown in Figure 5.3.

EG_{20} and EG_{40} SAMs were made by functionalizing the surface with azido-EG_{20} linkers in the click reaction, or by co-immobilizing thiol-EG_{20} or thiol-EG_{40} linkers during the enzyme binding step. 1% thiol-EG_{40} (Nanocs, PG1-TH-2K, 2000 MW average) surfaces were co-immobilized (1%) with NfsB on 1:10 EG_3MAL:EG_3-OH functionalized beads. The co-immobilization step was performed overnight at 4 °C with gentle agitation. 10% thiol-EG_{40} surfaces were made in the same manner as above, with the exception that it was co-immobilized with NfsB at 10%. 1% azido-

EG_{20} surfaces were made on silane-alkyne functionalized glass beads. The click reaction contained 1.2 nmol azido-EG_3-maleimide, 0.108 nmol azido-EG_{20} (Creative PEG works, mPEG-Azide MW 1K), 10.7 nmol azido-EG_3-OH per gram of beads functionalized. 10% azido-EG_{20} surfaces were also made on silane-alkyne functionalized glass beads. The click reaction contained 1.2 nmol azido-EG_3-MAL, 1.08 nmol azido-EG_{20} (Creative PEG works, mPEG-Azide MW 1K), 9.72 nmoles azido-EG_3-OH per gram of beads functionalized. After the click reactions were complete, beads were rinsed with DMSO (3 times), followed by rinsing with DI water (3 times). The beads were incubated for at least an hour with 0.5 M EDTA to get rid of excess copper, then washed with phosphate buffer (PBS) (100 mM phosphate, 300 mM NaCl, pH 7.5).

5.8 Enzyme Immobilization

Enzyme samples were prepared for immobilization by treatment with TCEP (1mM). Enzyme was bound to prepared surfaces at 5μM in PBS at 4 °C, shaking overnight. After binding, excess enzyme was rinsed away with PBS (3 times) followed by 3 rinses with 5% Tween-20 in PBS to eliminate non-specific binding. Tween-20 was rinsed away with 3 more PBS rinses. Excess copper from the click reaction present in bead samples interferes with the enzyme concentration measurement. To eliminate this interference, beads were incubated with 0.5M EDTA (pH 8.0) for 1 hour to chelate excess copper. The EDTA was then removed with 3 more PBS rinses. Immobilized enzyme samples were made fresh daily.

5.9 Immobilized Enzyme Concentration

Immobilized enzyme concentrations were measured by the micro bicinchoninic acid assay (BCA)(Figure 5.4). The micro-BCA assay solution comprises

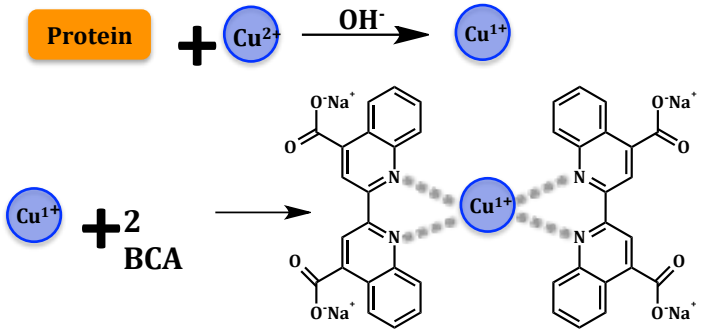

Figure 5.4. BCA Reaction Scheme
Diagram of bicinchoninic acid assay reaction used to determine immobilized protein concentrations

a mixture of 3 reagents. BCA reagent A contains 0.65 M sodium carbonate and 82 mM tartrate at pH 11.25. BCA reagent B contains 116 mM bicinchoninic acid in DI water. BCA reagent C contains 160 mM copper sulfate in DI water. Micro-BCA assay solution is made of 25:25:1 (v/v/v) with reagents A:B:C and was made fresh daily. Bead samples to be measured were re-suspended in 250µL PBS and mixed via vortex with 250µL micro-BCA assay solution. Samples were incubated for 15 minutes at 60 °C, then cooled to room temperature. Samples were mixed by vortex before reading the absorbance at 562nm. A standard curve was employed to make concentration calculations. For ng enzyme/mg bead surface coverage values, the quantity of enzyme was measured and then the beads were dried overnight in a drying oven before recording mass.

5.10 Surface Coverage

Parameters for the definition of a monolayer were calculated based on a 50 Å diameter of NfsB. A diffuse monolayer was defined as one enzyme per 10,000 Å^2, which is equivalent to 26 ng enzyme per mg of beads. A tightly packed monolayer was defined as 4 enzymes per 10,000 Å^2, which is equivalent to 102 ng enzyme per mg of beads (Figure 5.5). Beads for surface coverage experiments were prepared

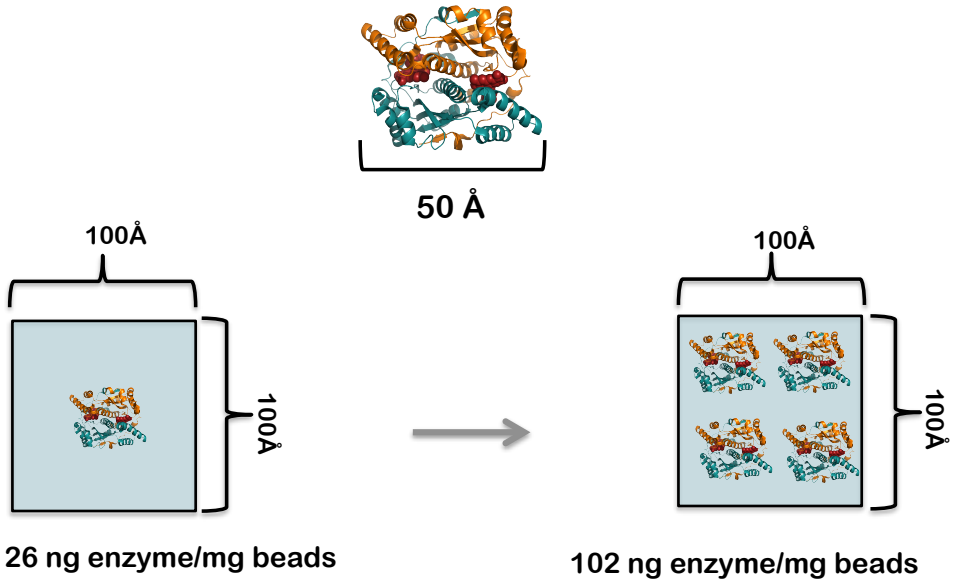

Figure 5.5. Diagram of Monolayer Limits
Diagram of defining limits for a monolayer and structure indicating the approximate diameter. One enzyme in 10,000 Å^2 being defined as a diffuse monolayer and being equivalent to 26 ng enzyme/mg beads. Four enzymes in 10,000 Å^2 is defined as a tightly packed monolayer and is equivalent to 102 ng enzyme/mg beads.

exactly as described above with alkyne functionalization followed by a click reaction with azido-EG$_3$-MAL and azido-EG$_3$-OH. Enzyme surface coverage was changed by increasing or reducing the enzyme concentration in the enzyme binding step. Enzyme was bound to bead samples in PBS at 4°C with shaking overnight. The surface coverage resulting from different binding concentrations is shown in Figure

5.6. It is important to note that the surface coverage is construct dependent, so to obtain the same surface coverage does not mean the same binding concentration was used.

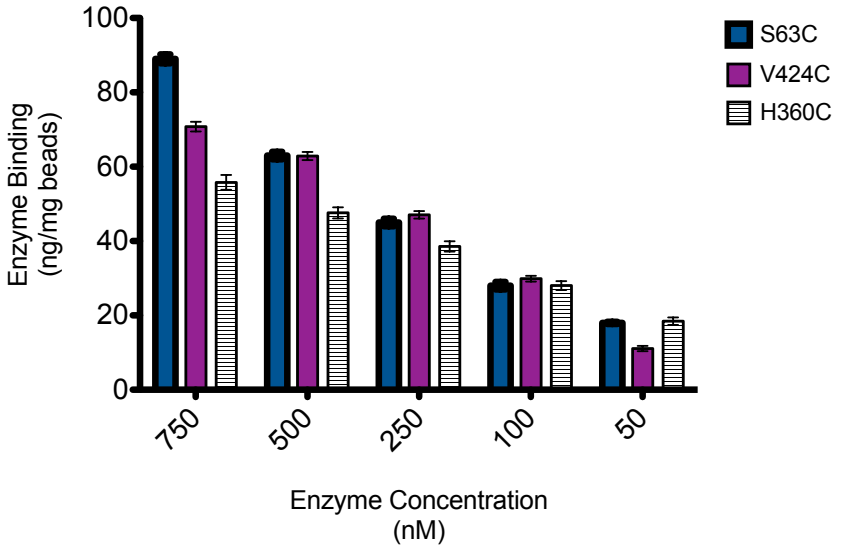

Figure 5.6. Surface Binding Data
Amount of enzyme bound to bead surfaces as a function of protein concentration in the binding reaction.

5.11 Enzyme Assay in Solution

Enzyme samples were removed from -80 °C storage and thawed on ice. Buffer exchange was performed (10,000 MW Amicon Centrifugal Filters) to remove storage buffer and replace with PBS. Enzyme samples were diluted appropriately. Each activity assay contained: NADH (160μM), 4-nitrobenzenesulfonamide(500μM) and enzyme in PBS. NADH was made fresh daily at a stock concentration of 1.6mM in PBS. 4-Nitrobenzenesulfonamide stock was made in DMSO due to greater solubility in this solvent. Enzyme concentrations were changed appropriately. Samples were mixed with NADH and 4-nitrobenzenesulfonamide in PBS, and the reaction was started with the addition of enzyme. Samples were thoroughly mixed

via vortex or pipet. UV absorbance at 340nm was collected every 10 seconds between 2 and 5 minutes depending on the assay.

5.12 Immobilized Enzyme Assay

Prepared enzyme bead samples were rinsed with PBS and then the supernatant was removed by decanting. The activity assay solution (NADH (160 μM), 4-nitrobenzenesulfonamide (500 μM), in PBS, pH 7.5)) was then added to the bead sample. A zero time point sample was immediately removed and absorbance measured at 340nm. The sample was replaced into the reaction and the reaction mixture shaken. Samples were shaken so the beads remained suspended. A sample was removed for an absorbance measurement every 30 seconds for 2 to 4 minutes. After the activity assays were complete, the bead samples were then washed with PBS and the protein concentration was measured using the micro-BCA reaction.

5.13 Thermal Stability Assay

To assess enzyme stability, thermal stability assays were performed both in free solution and on immobilized enzyme samples. For enzyme samples in solution, the enzyme stock was buffer exchanged to remove storage buffer and replaced with PBS using centrifugal filter unit (Amicon, 10000 MW). FMN (100 μM) was added to enzyme stocks and they were placed in PCR tubes. The samples were heated between 20 °C to 65 °C for 5 minutes in a thermocycler. The samples were then brought to room temperature for at least 10 minutes. The remaining activity was then measured following the parameters for the enzyme assay.

Prepared immobilized enzyme bead samples were re-suspended in PBS with 100 μM FMN. Samples were then heated between 20° to 65°C in PCR tubes using a thermocycler for 5 minutes. After heating, samples were brought to room temperature for 10 minutes, the remaining specific activity was then measured as described above for the immobilized enzyme assay.

$$y = A_2 + \frac{A_1 - A_2}{1 + exp\left(\frac{T\,½ - T}{slope}\right)}$$

Equation 1.
A_1 and A_2 are the upper and lower asymptotes and T ½ is the temperature at which one have the activity remains

To determine T ½ the data were fit to equation 1, with A_1 representing the upper and A_2 representing the lower asymptotes of enzyme activity. T ½ is the temperature where one half of the initial activity remains.

Chapter 6

Conclusion and Future Directions

6.1 Conclusion

Enzymes are unmatched in their ability to increase the rate of reactions. The mild reaction conditions under which they operate and high substrate specificity make enzymes particularly attractive as catalysts for commercial applications. Despite their catalytic power; there are significant drawbacks to using enzymes in industrial or medical settings. They are generally expensive to produce and expensive to re-purify from reaction mixtures. Their activity can be reduced by product inhibition in some cases. The half-life of an enzyme can be limited due to unfolding, oxidation, or proteolysis.

Immobilization of enzymes on solid supports has been found to overcome some of these limitations, and much work has been done to establish different types of immobilization and immobilization supports, as discussed in Chapter 1. Far less work has been done to investigate, on a molecular level, the relationship between orientation, catalytic activity, and stability on a well-defined single orientation chemical linkage system. The detailed understanding that may arise from such studies should prove valuable in designing improved immobilization strategies that better preserve enzyme stability and enhance catalytic activity.

6.1.2 Determining Effect of Immobilization Orientation on Activity of NfsB

One aspect of enzyme immobilization that has seldom been investigated is the effect of orientation on the activity of an immobilized enzyme. This research has aimed to investigate whether orientation plays a role in the activity of immobilized enzymes. To address this question we used maleimide terminated SAMs on glass surfaces to covalently immobilize NfsB, a model enzyme, through engineered surface cysteine residues. Two NfsB variants were created: one placing a cysteine residue at position 360 and the other at position 424. Immobilization through position 360 oriented the active sites perpendicular to the surface while immobilization through 424 oriented the active sites parallel to the surface. These orientations were confirmed using SFG and activity measurements made in solution confirmed that introducing the cysteine residues did not change the activity or folding of the enzyme.

Octadecyltrichlorosilane (OTS) was used as a SAM surface for non-specific physical adsorption to show that non-specific physical adsorption produces significantly less specific activity than enzyme immobilized with maleimide SAM surfaces. The specific activity of NfsB immobilized on a maleimide SAM surface and the specific activity on the OTS surface were 5.8±0.5 μM/min/μg enzyme and 1.4±0.2 μM/min/μg enzyme, respectively. However, the specific activity of the two NfsB variants H360C and V424C were the same. These results support the conclusion that specifically-oriented, single covalent linkage immobilization

provides a significant advantage in specific activity as compared to non-specific adsorption. This is likely because non-specific adsorption causes multiple unfavorable orientations and partial unfolding of the enzyme on the surface. These results agree with examples from other groups and also with results from other studies performed in our lab. Studies performed by Dr. Tadeusz Ogorzalek on betagalactosidase had similar results with a higher specific activity achieved when the enzyme was immobilized to a maleimide-SAM surface as compared to OTS.

The two orientation variants tested in these studies did not differ in their specific activities when covalently tethered to the surface. This indicates that orientation effects don't play a significant role in the changing the specific activity of NfsB. It is also important to note here the role that the molecular structure of the linkers plays in difference in the activity of activity the immobilized enzymes. The siliane-EG_4-maleimide linker gave a specific activity of 14±1 μM/min/μg enzyme for H360C and 7±2 μM/min/μg enzyme for V424C, while the EG_3-maleimide click linker showed no difference between the two variants. It is important to not that this activity was on a maleimide only SAM surface so the difference in specific activity could be attributed to hydrophobic effects reducing activity on the V424C variant. These results show that the surface-protein interactions are the most important for modulating the specific activity of immobilized enzyme.

6.1.3 Effects of Attachment Site and Surface Composition on Immobilized NfsB Activity and Stability

These experiments were performed to gain a better understanding of the effects that attachment site and surface composition have on the activity and stability of immobilized enzyme. We explored the effects of surface properties on enzyme stability and activity by creating mixed SAM surfaces, using alcohol- or methyl-terminated PEG surface coatings doped with the maleimide-terminated linker. We examined the effect of attachment point by making a new NfsB variant with the surface cysteine positioned in an α-helix instead of a loop region and the thermal stability of this variant was measured.

Placing the anchoring cysteine site on a helix region did not add any stability to the enzyme in our experiments and it also did not affect the specific activity in this case. We hypothesized that a helix anchor point would increase the immobilized enzyme's stability by reducing protein interactions with the surface through greater protein-linker rigidity. In experiments performed on beta-galactosidase it was shown that stability was increased when immobilized through a helix anchor point by increasing the T ½. This was not reproduced using NfsB. This supports the idea that some qualities of immobilized enzymes appear to be enzyme specific and not conform to an obvious trend. One quality the helix cysteine NfsB variant displayed was that it bound more readily to the glass surface.

SAM surfaces were constructed with mixtures of maleimide-terminated PEGS and varying rations of alcohol- or methyl-terminated PEG. We found that with both

alcohol and methyl terminated linkers the 1:10 ratio of maleimide terminated linker to alcohol or methyl terminated linkers gave the highest specific activity and in all cases the alcohol surface had higher specific activity than the methyl terminated surface. These results exemplify the importance of the surface itself. The interactions generated by the surface towards the immobilized enzyme play a large role in the catalytic activity and also suggests that the effects may be related to the hydrophobicity of the surface with the more hydrophilic surface supporting higher specific activity.

When we made a range of surfaces from more hydrophobic to more hydrophilic we found that this did not affect the T ½ of the immobilized enzyme, but did affect the specific activity. This again supports the idea that the surface has an important role and our results show that a more hydrophilic surface is better for catalytic activity. Less catalytic activity on hydrophobic surfaces suggests that there are hydrophobic interactions between the protein and the surface that are too strong and could be distorting the enzyme structure. The hydrophilic surfaces eliminate these hydrophobic interactions and restore some enzyme activity.

6.1.4 Stability Through Surface Crowding and Co-immobilization

We explored the effect of surface crowding on enzyme activity by changing the density of enzyme immobilized on the surface and also by adding higher

molecular weight PEG linkers to the surface with the immobilized enzyme. First we established a monolayer as being between 26 ng enzyme per mg beads and 102 ng enzyme per mg beads. Then we measured specific activity and T ½ for H360C, V424C and S63C NfsB variants. We found that for V424C and S63C the specific activity and the T ½ were unaffected by the surface coverage. For H360C we found a slight decrease in specific activity with a decrease in surface coverage. We also found a decrease in T ½ for lower surface coverage. These results suggest an orientation dependent effect. The H360C NfsB variant orients the active sites perpendicular to the surface and facing its neighbor's active site. We hypothesize that the reason for this effect is that at lower surface density the enzyme and surface are interacting strongly enough to reduce activity and stability. As the surface density increases these surface-protein interactions are blocked by the neighboring immobilized protein. These results are at odds with the results found by Liu and coworkers using gold nanoparticles. In their experiments, they found that surface density did not affect activity as long as the anchoring residue was located far from the active site. In instances where the anchoring site was located near an active site the surface density influenced the activity significantly[28]. In our experiments the V424C and S63C variants have the anchor site farthest from the active sites yet their specific activities remain the same over different surface densities.

Higher molecular weight PEG SAM surfaces were made to determine if co-immobilization provided a stabilizing effect to immobilized NfsB. We found that for both EG_{20} and EG_{40} co-immobilized either H360C or V424C NfsB variants there weren't any significant changes in T ½. For both EG_{20} and EG_{40} co-immobilized with

NfsB we observed a decrease in specific activity. The reduction is a bit greater for the V424C NfsB variant, which suggests that the longer PEG linkers could be blocking access to the active site facing solution.

6.2 Future Directions

We tested a range of hydrophobicity and the effects on activity and stability. It would be interesting to expand on these experiments by making SAM surfaces that are more hydrophobic than the methyl terminated surfaces detailed here. We hypothesize that activity will be reduced as hydrophobicity increases. This would prove that the hydrophobicity of the surface is the most important surface quality for maintaining activity. Other types of hydrophilic surfaces could be tested as well including acidic surfaces. Specific activity could increase even further with increasing the hydrophilic nature of the surface.

Beyond just hydrophobicity, there are many options available for making SAM surfaces. We learned that the surface has a large effect on activity, so the next step would be to test different surface characteristics. The surface could be made more hydrophobic than with a methyl-terminated linker and more hydrophilic than the alcohol-terminated linker. Another surface property to change would be the

charge, which could be made positive or negative. Some promising results have been seen with zwitterionic surfaces as well, so that would be another option.

The temperature curves we used to measure T ½ are only one way to look at stability. There are other ways including using organic solvents and other harsh conditions that could be used in industrial applications. It would be an interesting experiment to test some of these immobilized enzymes in other types of stability assays. In these experiments, immobilized enzyme would be exposed to an organic solvent such as dimethylsulfoxide and the remaining activity would be measured. Alternatively, in a water miscible solvent like dimethylsulfoxide it is possible that activity could be measured in a solution of dimethylsulfoxide and water. Stability can also be measured as re-usability or longevity of storage. For these experiments an immobilized enzyme sample would be tested for activity after storage at 4° C or repeated activity measurements on the same immobilized enzyme sample to determine the possible number of re-uses. Another idea that could be utilized is the co-immobilization with PEG. PEG is available in many sizes and even branched versions. It would be interesting to try co-immobilizing with branched PEG and measure activity in organic solvent environments to see if there is a stabilizing effect added.

Finally, there are some questions to be answered in regards to the surface crowding experiments detailed in chapter 4. More experiments could be done to determine the reason for the orientation effect for H360C NfsB on a sparse monolayer. For example, another variant could be engineered to orient the active sites similarly to H360C and determine if the T ½ and specific activity decrease is

consistent with the H360C variant. If the same results were found with this new variant, it could be concluded that the effect is a consequence of the orientation of the active sites. If the results were not reproduced it could be concluded that the effect was due to the specific anchor site.

References

1. Radzicka, A. & Wolfenden, R. A proficient enzyme. *Science* **267,** 90–93 (1995).
2. Garcia-Galan, C., Berenguer-Murcia, ??, Fernandez-Lafuente, R. & Rodrigues, R. C. Potential of different enzyme immobilization strategies to improve enzyme performance. *Adv. Synth. Catal.* **353,** 2885–2904 (2011).
3. Liang, J. F., Li, Y. T. & Yang, V. C. Biomedical application of immobilized enzymes. *J. Pharm. Sci.* **89,** 979–990 (2000).
4. Busto, M. D., García-Tramontín, K. E., Ortega, N. & Perez-Mateos, M. Preparation and properties of an immobilized pectinlyase for the treatment of fruit juices. *Bioresour. Technol.* **97,** 1477–1483 (2006).
5. Spagna, G., Pifferi, P. G. & Martino, A. Pectinlyase immobilization on epoxy supports for application in the food processing industry. *J. Chem. Technol. Biotechnol.* **57,** 379–385 (1993).
6. Alkorta, I., Garbisu, C., Llama, J. & Serra, J. L. Immobilization of pectin lyase from. *Enzyme* **229,** 141–146 (1996).
7. Hanisch, W. H., Rickard, P. A. D. & Nyo, S. Poly(methoxygalacturonide) lyase immobilized via titanium onto solid supports. *Biotechnol. Bioeng.* **20,** 95–106 (1978).
8. Katchalski-Katzir, E. & Kraemer, D. M. Eupergit® C, a carrier for immobilization of enzymes of industrial potential. *J. Mol. Catal. - B Enzym.* **10,**

157–176 (2000).

9. Bhosale, S. H., Rao, M. B. & Deshpande, V. V. Molecular and industrial aspects of glucose isomerase. *Microbiol. Rev.* **60,** 280–300 (1996).

10. Tischer, W. & Wedekind, F. Immobilized Enzymes: Methods and Applications. *Biocatal. - From Discov. to Appl.* **200,** 95–126 (1999).

11. Doretti, L., Ferrara, D., Gattolin, P. & Lora, S. Covalently immobilized enzymes on biocompatible polymers for amperometric sensor applications. *Biosens. Bioelectron.* **11,** 365–373 (1996).

12. Kudo, H. *et al.* Glucose sensor using a phospholipid polymer-based enzyme immobilization method. *Anal. Bioanal. Chem.* **391,** 1269–1274 (2008).

13. Matsumoto, K. *et al.* Fluorometric determination of carnitine in serum with immobilized carnitine dehydrogenase and diaphorase. *Clin. Chem.* **36,** 2072–2076 (1990).

14. Eggenstein, C. *et al.* A disposable biosensor for urea determination in blood based on an ammonium-sensitive transducer. *Biosens. Bioelectron.* **14,** 33–41 (1999).

15. Gilmartin, M. A. T. & Hart, J. P. Fabrication and characterization of a screen-printed, disposable, amperometric cholesterol biosensor. *Analyst* **119,** 2331–2336 (1994).

16. Yoo, E.-H. & Lee, S.-Y. Glucose Biosensors: An Overview of Use in Clinical Practice. *Sensors* **10,** 4558–4576 (2010).

17. Mateo, C., Palomo, J. M., Fernandez-Lorente, G., Guisan, J. M. & Fernandez-Lafuente, R. Improvement of enzyme activity, stability and selectivity via

immobilization techniques. *Enzyme Microb. Technol.* **40,** 1451–1463 (2007).

18. Jesionowski, T., Zdarta, J. & Krajewska, B. Enzyme immobilization by adsorption: A review. *Adsorption* **20,** 801–821 (2014).
19. Hernandez, K. & Fernandez-Lafuente, R. Control of protein immobilization: Coupling immobilization and site-directed mutagenesis to improve biocatalyst or biosensor performance. *Enzyme Microb. Technol.* **48,** 107–122 (2011).
20. Geetha, S., Rao, C. R. K., Vijayan, M. & Trivedi, D. C. Biosensing and drug delivery by polypyrrole. *Anal. Chim. Acta* **568,** 119–125 (2006).
21. Ekanayake, E. M. I. M., Preethichandra, D. M. G. & Kaneto, K. Polypyrrole nanotube array sensor for enhanced adsorption of glucose oxidase in glucose biosensors. *Biosens. Bioelectron.* **23,** 107–113 (2007).
22. Chen, Y. Z., Yang, C. T., Ching, C. B. & Xu, R. Immobilization of lipases on hydrophobilized zirconia nanoparticles: Highly enantioselective and reusable biocatalysts. *Langmuir* **24,** 8877–8884 (2008).
23. Sassolas, A., Blum, L. J. & Leca-Bouvier, B. D. Immobilization strategies to develop enzymatic biosensors. *Biotechnol. Adv.* **30,** 489–511 (2012).
24. Sohail, M. & Adeloju, S. B. Electroimmobilization of nitrate reductase and nicotinamide adenine dinucleotide into polypyrrole films for potentiometric detection of nitrate. *Sensors Actuators, B Chem.* **133,** 333–339 (2008).
25. Datta, S., Christena, L. R. & Rajaram, Y. R. S. Enzyme immobilization: an overview on techniques and support materials. *3 Biotech* 1–9 (2012). doi:10.1007/s13205-012-0071-7

26. Zhai, D. *et al.* Highly sensitive glucose sensor based on pt nanoparticle/polyaniline hydrogel heterostructures. *ACS Nano* **7,** 3540–3546 (2013).

27. Jeong, M. L. *et al.* Direct immobilization of protein G variants with various numbers of cysteine residues on a gold surface. *Anal. Chem.* **79,** 2680–2687 (2007).

28. Liu, F. *et al.* Modulating the activity of protein conjugated to gold nanoparticles by site-directed orientation and surface density of bound protein. *ACS Appl. Mater. Interfaces* **7,** 3717–3724 (2015).

29. Cabrita, J. F., Abrantes, L. M. & Viana, A. S. N-Hydroxysuccinimide-terminated self-assembled monolayers on gold for biomolecules immobilisation. *Electrochim. Acta* **50,** 2117–2124 (2005).

30. Zimmermann, J. L., Nicolaus, T., Neuert, G. & Blank, K. Thiol-based, site-specific and covalent immobilization of biomolecules for single-molecule experiments. *Nat. Protoc.* **5,** 975–985 (2010).

31. Ghosh, S. S., Kao, P. M., McCue, a W. & Chappelle, H. L. Use of maleimide-thiol coupling chemistry for efficient syntheses of oligonucleotide-enzyme conjugate hybridization probes. *Bioconjug. Chem.* **1,** 71–76 (1990).

32. Liese, A. & Hilterhaus, L. Evaluation of immobilized enzymes for industrial applications. *Chem. Soc. Rev.* **42,** 6236–49 (2013).

33. Hanefeld, U., Gardossi, L. & Magner, E. Understanding enzyme immobilisation. *Chem Soc Rev* **38,** 453–468 (2009).

34. Rodrigues, R. C., Ortiz, C., Berenguer-Murcia, Á., Torres, R. & Fernández-

Lafuente, R. Modifying enzyme activity and selectivity by immobilization. *Chem. Soc. Rev.* **42,** 6290–6307 (2013).

35. Mateo, C. *et al.* Epoxy Sepabeads: A novel epoxy support for stabilization of industrial enzymes via very intense multipoint covalent attachment. *Biotechnol. Prog.* **18,** 629–634 (2002).

36. Wei, S. & Knotts IV, T. A. A coarse grain model for protein-surface interactions. *J. Chem. Phys.* **139,** (2013).

37. Moskovitz, Y. & Srebnik, S. Conformational changes of globular proteins upon adsorption on a hydrophobic surface. *Phys. Chem. Chem. Phys.* **16,** 11698–11707 (2014).

38. Loong, B. K. & Knotts, T. A. Communication: Using multiple tethers to stabilize proteins on surfaces. *J. Chem. Phys.* **141,** (2014).

39. Zhao, H. Methods for stabilizing and activating enzymes in ionic liquids - A review. *J. Chem. Technol. Biotechnol.* **85,** 891–907 (2010).

40. Houseman, B. T., Gawalt, E. S. & Mrksich, M. Maleimide-functionalized self-assembled monolayers for the preparation of peptide and carbohydrate biochips. *Langmuir* **19,** 1522–1531 (2003).

41. Zenno, S., Koike, H., Tanokura, M. & Saigo, K. Gene cloning, purification, and characterization of NfsB, a minor oxygen-insensitive nitroreductase from Escherichia coli, similar in biochemical properties to FRase I, the major flavin reductase in Vibrio fischeri. *J. Biochem.* **120,** 736–44 (1996).

42. Emptage, C. D., Knox, R. J., Danson, M. J. & Hough, D. W. Nitroreductase from Bacillus licheniformis: A stable enzyme for prodrug activation. *Biochem.*

Pharmacol. **77,** 21–29 (2009).

43. Parkinson, G. N., Skelly, J. V. & Neidle, S. Crystal structure of FMN-dependent nitroreductase from Escherichia coli B: A prodrug-activating enzyme. *J. Med. Chem.* **43,** 3624–3631 (2000).

44. Bolivar, J. M., Consolati, T., Mayr, T. & Nidetzky, B. Shine a light on immobilized enzymes: Real-time sensing in solid supported biocatalysts. *Trends Biotechnol.* **31,** 194–203 (2013).

45. Wang, J., Buck, S. M. & Chen, Z. Sum Frequency Generation Vibrational Spectroscopy Studies on Protein Adsorption. *J. Phys. Chem. B* **106,** 11666–11672 (2002).

46. Wang, J. *et al.* Detection of amide I signals of interfacial proteins in situ using SFG. *J. Am. Chem. Soc.* **125,** 9914–9915 (2003).

47. Shen, L. *et al.* Surface orientation control of site-specifically immobilized nitro-reductase (NfsB). *Langmuir* **30,** 5930–5938 (2014).

48. Fu, J., Reinhold, J. & Woodbury, N. W. Peptide-modified surfaces for enzyme immobilization. *PLoS One* **6,** 2–7 (2011).

49. Wong, L. S., Khan, F. & Micklefield, J. Selective covalent protein immobilization: Strategies and applications. *Chem. Rev.* **109,** 4025–4053 (2009).

50. Iyer, P. V. & Ananthanarayan, L. Enzyme stability and stabilization-Aqueous and non-aqueous environment. *Process Biochem.* **43,** 1019–1032 (2008).

51. DiCosimo, R., McAuliffe, J., Poulose, A. J. & Bohlmann, G. Industrial use of immobilized enzymes. *Chem. Soc. Rev.* **42,** 6437 (2013).

52. Chauhan, S., Vohra, A., Lakhanpal, A. & Gupta, R. Immobilization of Commercial Pectinase (Polygalacturonase) on Celite and Its Application in Juice Clarification. *J. Food Process. Preserv.* **39,** 2135–2141 (2015).

53. Ogorzalek, T. L. *et al.* Molecular-Level Insights into Orientation-Dependent Changes in the Thermal Stability of Enzymes Covalently Immobilized on Surfaces. *Langmuir* **31,** 6145–6153 (2015).

54. Caseli, L., Furriel, R. P. M., De Andrade, J. F., Leone, F. A. & Zaniquelli, M. E. D. Surface density as a significant parameter for the enzymatic activity of two forms of alkaline phosphatase immobilized on phospholipid Langmuir-Blodgett films. *J. Colloid Interface Sci.* **275,** 123–130 (2004).

55. Zoungrana, T., Findenegg, G. & Norde, W. Structure, Stability, and Activity of Adsorbed Enzymes. *J. Colloid Interface Sci.* **190,** 437–48 (1997).

56. Sheldon, R. A. Enzyme immobilization: The quest for optimum performance. *Adv. Synth. Catal.* **349,** 1289–1307 (2007).

57. Zhang, M., Li, X. H., Gong, Y. D., Zhao, N. M. & Zhang, X. F. Properties and biocompatibility of chitosan films modified by blending with PEG. *Biomaterials* **23,** 2641–2648 (2002).

58. Hinds, K. D. & Kim, S. W. Effects of PEG conjugation on insulin properties. *Adv. Drug Deliv. Rev.* **54,** 505–530 (2002).

59. Abuchowski, A. & Davis, F. F. Preparation and properties of polyethylene glycol-trypsin adducts. *BBA - Protein Struct.* **578,** 41–46 (1979).

60. Gasteiger, E. *et al.* ExPASy: The proteomics server for in-depth protein knowledge and analysis. *Nucleic Acids Res.* **31,** 3784–3788 (2003).